© 2018. Published by The Company of Biologists Ltd | Development (2018) 145, dev163568. doi:10.1242/dev.163568

RESEARCH ARTICLE

Neurog3-dependent pancreas dysgenesis causes ectopic pancreas in *Hes1* mutant mice

Mette C. Jørgensen[1], Kristian H. de Lichtenberg[1], Caitlin A. Collin[1], Rasmus Klinck[2], Jeppe H. Ekberg[3], Maja S. Engelstoft[3], Heiko Lickert[4] and Palle Serup[1,*]

ABSTRACT

Mutations in *Hes1*, a target gene of the Notch signalling pathway, lead to ectopic pancreas by a poorly described mechanism. Here, we use genetic inactivation of *Hes1* combined with lineage tracing and live imaging to reveal an endodermal requirement for Hes1, and show that ectopic pancreas tissue is derived from the dorsal pancreas primordium. RNA-seq analysis of sorted E10.5 $Hes1^{+/+}$ and $Hes1^{-/-}$ Pdx1-GFP^{+} cells suggested that upregulation of endocrine lineage genes in $Hes1^{-/-}$ embryos was the major defect and, accordingly, early pancreas morphogenesis was normalized, and the ectopic pancreas phenotype suppressed, in $Hes1^{-/-}Neurog3^{-/-}$ embryos. In *Mib1* mutants, we found a near total depletion of dorsal progenitors, which was replaced by an anterior Gcg^{+} extension. Together, our results demonstrate that aberrant morphogenesis is the cause of ectopic pancreas and that a part of the endocrine differentiation program is mechanistically involved in the dysgenesis. Our results suggest that the ratio of endocrine lineage to progenitor cells is important for morphogenesis and that a strong endocrinogenic phenotype without complete progenitor depletion, as seen in *Hes1* mutants, provokes an extreme dysgenesis that causes ectopic pancreas.

KEY WORDS: Hes1, Ectopic pancreas, Neurog3, Morphogenesis

INTRODUCTION

Vertebrate organs form in a stereotypical manner that is based on patterning of embryonic tissues along the three axes of the body. Organ dysfunction can occur if the initial patterning events or the later growth, morphogenesis and cell differentiation processes go awry. Congenital malformations of the pancreas include ectopic pancreas, defined as pancreatic tissue lacking anatomic and vascular continuity with the main body of the gland, annular pancreas, where the ventral pancreas encircles the duodenum and occasionally causes duodenal obstruction, and pancreas divisum, where the ventral and dorsal pancreas fail to fuse (Tadokoro et al., 2011). Ectopic pancreas can develop at multiple sites including the stomach, duodenum and jejunum (Türkvatan et al., 2013), but little is known about the underlying genetic and developmental causes.

[1]NNF Center for Stem Cell Biology (DanStem), Faculty of Health and Medical Sciences, University of Copenhagen, DK-2200 Copenhagen, Denmark. [2]Novo Nordisk A/S, Department of User Research and Communication, Brennum Park 1, DK-3400 Hillerød, Denmark. [3]NNF Center for Basic Metabolic Research, Section for Metabolic Receptology, Laboratory for Molecular Pharmacology, Faculty of Health and Medical Sciences, University of Copenhagen, DK-2200 Copenhagen, Denmark. [4]Institute of Stem Cell Research, Helmholtz Zentrum München, 85764 Neuherberg, Germany.

*Author for correspondence (palle.serup@sund.ku.dk)

P.S., 0000-0002-0858-590X

Received 18 January 2018; Accepted 23 July 2018

The mouse pancreas develops from two primordia visible as thickenings of the posterior foregut epithelium around embryonic day (E) 9.0. The pancreatic buds are composed of multipotent pancreatic progenitor cells (MPCs) that express a cohort of transcription factors, including Hnf1β, Pdx1, Ptf1a, Nkx6-1, Sox9, Gata4 and Gata6, many of which have segregated to distinct tip and trunk compartments by ∼E14 (Bastidas-Ponce et al., 2017). The two buds grow independently until ∼E12.5, when they fuse to form a single organ connected to the digestive tract via the common bile duct. The ventral pancreas becomes associated with the duodenal loop, whereas the dorsal pancreas grows along the side of the stomach towards the spleen. At E14.5, the gastric lobe grows out from the base of the dorsal pancreas and wraps around the pylorus reaching towards the other side of the stomach (Hörnblad et al., 2011; Villasenor et al., 2010).

Some pancreatic malformations are coupled to loss-of-function mutations in developmental signalling pathways. For example, the Hedgehog family of signalling molecules play an important role in pancreas morphogenesis. Two genes of the Hedgehog family, sonic hedgehog (*Shh*) and indian hedgehog (*Ihh*), are expressed in partially overlapping patterns in the gut tube (Bitgood and McMahon, 1995; Echelard et al., 1993). *Shh* is expressed in endoderm adjacent to the pancreas but is excluded from pancreatic endoderm (Ahlgren et al., 1997; Apelqvist et al., 1997; Hebrok et al., 2000), and although *Ihh* is co-expressed with *Shh* in many endodermal domains, it is also expressed at a low level in the pancreas (Hebrok et al., 2000). Notably, null mutations in both genes cause annular pancreas, a ventral pancreas malformation, albeit with variable penetrance, depending on the genetic background (Hebrok et al., 2000; Ramalho-Santos et al., 2000). Comparably, loss of the transcription factor Hes1, the gene for which is a target and effector of Notch signalling in the pancreas, causes ectopic pancreas formation (Fukuda et al., 2006; Sumazaki et al., 2004). The Notch pathway is best known for its role in regulating differentiation of both endocrine and exocrine cell types in the pancreas. Loss-of-function mutations in the Notch pathway cause accelerated and excessive differentiation of pancreatic endocrine cells, by de-repression of the proendocrine gene *Neurog3*, which combined with reduced proliferation of MPCs results in a hypoplastic pancreas (Apelqvist et al., 1999; Fujikura et al., 2006, 2007; Jensen et al., 2000). More recently, loss of the Notch signalling components Mib1 and Hes1, as well as expression of dominant-negative Maml1, was shown to also cause the loss of the Nkx6-1^{+} bipotent duct/endocrine progenitors and an excess of Ptf1a^{+} pre-acinar cells at the secondary transition (Afelik et al., 2012; Horn et al., 2012). Conversely, overexpression of constitutively active Notch1 in the pancreas epithelium promotes an Nkx6-1^{+} fate, but prevents differentiation of endocrine and acinar cells (Hald et al., 2003; Murtaugh et al., 2003; Schaffer et al., 2010). A *Hes1* null mutation is notable among the different

Development (2018) 145, dev163568. doi:10.1242/dev.163568

Notch pathway mutations, as the only mutation reported to cause gall bladder agenesis along with ectopic pancreas in the common bile duct (Sumazaki et al., 2004), and a later study also revealed ectopic pancreas tissue in the stomach and duodenum (Fukuda et al., 2006). Further investigations of the malformations in the common bile duct revealed that Hes1 acts in conjunction with the transcription factor Sox17 to define the pancreato-biliary boundary in the ventral posterior foregut (Spence et al., 2009). The patches of ectopic pancreas located outside the biliary system in *Hes1* nulls were suggested to arise from re-specified stomach or intestinal endoderm, after somatic loss of additional Hes family genes, but this idea was not tested (Fukuda et al., 2006).

Here, we show that ectopic pancreas tissue positioned outside the biliary system in *Hes1* mutants is located dorsally and anterior to the pancreas proper and, in extreme cases, approaches the level of the oesophagotracheal septum. We show that conditional deletion of *Hes1* in the endoderm recapitulates the ectopic pancreas phenotype seen in *Hes1* nulls, suggesting that Hes1 is specifically required in the endoderm. Significantly, we show by lineage tracing that the anterior ectopic pancreas tissue is derived from the E8.5 dorsal pancreas primordium, which is specified normally in *Hes1* mutants but becomes dysgenic at later stages. Remarkably, we found that dorsal bud morphogenesis was normalized, and ectopic pancreas formation suppressed, in *Hes1*$^{-/-}$*Neurog3*$^{-/-}$ double mutants. We find that mutations in two other Notch pathway genes, *Dll1* and *Mib1*, caused either no sign of ectopic pancreas (*Dll1*) or an anterior extension of the dorsal pancreas made up entirely by endocrine cells and devoid of progenitors (*Mib1*). Because *Dll1* and *Mib1* mutants have respective weaker and stronger endocrinogenic phenotypes than *Hes1* mutants, our results suggest that the ratio between MPCs and cells of the endocrine lineage is important for normal morphogenesis. Thus, a huge excess of endocrine-fated cells without complete progenitor depletion, as seen exclusively in *Hes1* mutants, appears to provoke ectopic pancreas formation by disrupting normal morphogenesis.

RESULTS

Progressive rostral extension of ectopic pancreas tissue in *Hes1* mutants

To examine how ectopic pancreas formation is manifested in *Hes1* mutants we first evaluated the structure of the developing pancreas and surrounding gut regions from E8.5 to E12.5 by whole-mount immunofluorescence (IF). The dorsal and ventral pancreas anlage, marked by expression of Pdx1, appeared normal in E8.5 *Hes1*$^{+/+}$ and *Hes1*$^{-/-}$ embryos, whereas Sox9^{+} cells were confined to the dorsal anlage in both genotypes (Fig. S1). In contrast, the dorsal anlage of E9.5 *Hes1*$^{-/-}$ embryos displayed an irregular, saddle-like shape with Pdx1^{Hi} cells extending in both anterior and posterior directions. The bud itself appeared flattened and, as expected (Ahnfelt-Rønne et al., 2012; Jensen et al., 2000), a vast excess of Neurog3^{+} and glucagon^{+} cells were present compared with wild type (Fig. 1A,B). A flattened bud was also seen in E10.5 *Hes1*$^{-/-}$ embryos but, remarkably, we also found ectopic tissue along the entire dorsal aspect of the stomach (Fig. 1C,D). The ectopic tissue contained Pdx1^{+}Ptf1a^{+}Nkx6-1^{+} cells, indicating a pancreatic MPC fate, as well as Neurog3^{+} endocrine precursors and endocrine cells expressing glucagon and PYY, as is typical for E10.5 embryos (Upchurch et al., 1994) (Fig. 1C,D, Fig. 2I, Fig. 5C, Fig. S2). At E11.5, the ectopic pancreas tissue is extending more anteriorly, forming a continuous cord from the flattened dorsal pancreas bud along the dorsal stomach endoderm and the posterior oesophagus

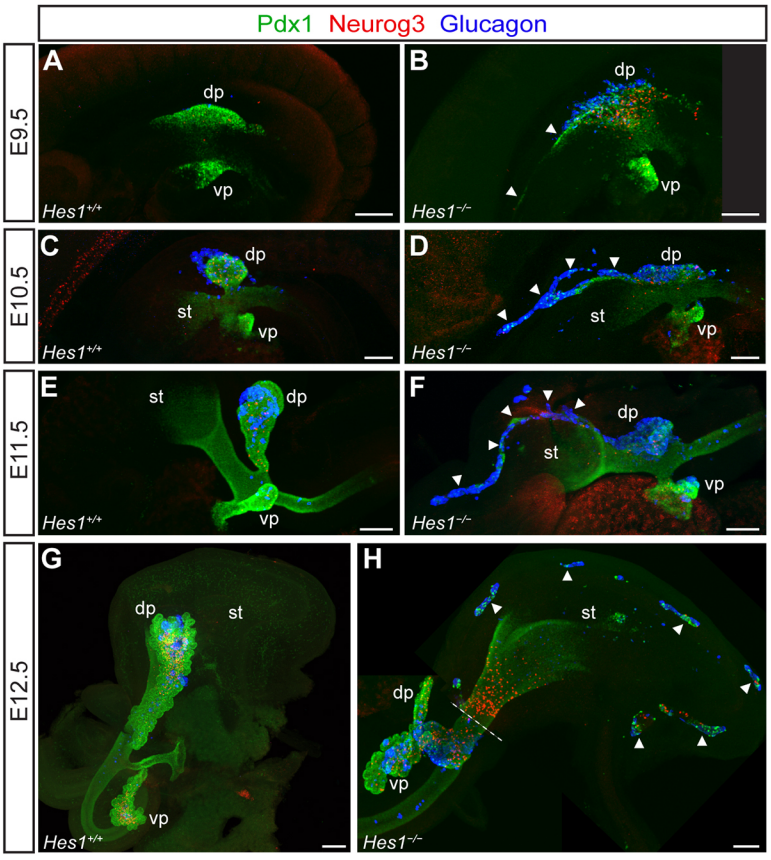

Fig. 1. Development of ectopic pancreas in *Hes1* mutant embryos. (A-H) Projections of E9.5 (A,B), E10.5 (C,D), E11.5 (E,F) and E12.5 (G,H) pancreatic primordia from *Hes1*$^{+/+}$ (A,C,E,G) and *Hes1*$^{-/-}$ (B,D,F,H) embryos, showing Pdx1, Neurog3 and glucagon by whole-mount IF. Arrowheads in B, D and F indicate the anterior extension of the dorsal pancreas. (H) Composite image with a dashed line indicating the level at which the image is stitched. Arrowheads indicate patches of ectopic pancreas tissue located in the dorsal part of the stomach. dp, dorsal pancreas; st, stomach; vp, ventral pancreas. Scale bars: 100 µm.

Development (2018) 145, dev163568. doi:10.1242/dev.163568

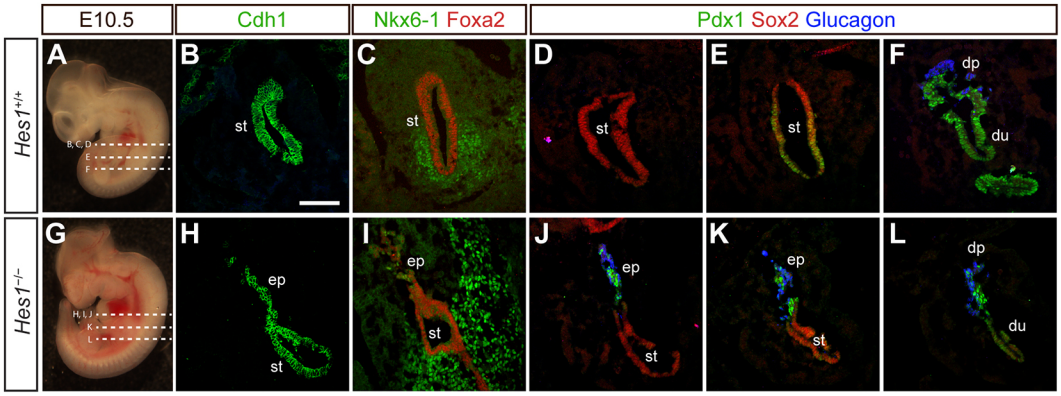

Fig. 2. Ectopic pancreas epithelium is contiguous with stomach epithelium. (A-L) Whole E10.5 embryo images of *Hes1*$^{+/+}$ (A) and *Hes1*$^{-/-}$ (G) with dashed lines indicating the plane of the sections in B-F and H-L. IF analysis of stomach and pancreas regions in *Hes1*$^{+/+}$ (B-F) and *Hes1*$^{-/-}$ (H-L) embryos, showing Cdh1 (B,H), Foxa2 and Nkx6-1 (C,I), or Pdx1, Sox2 and glucagon (D-F,J-L). Dorsal is up. dp, dorsal pancreas; du, duodenum; ep, ectopic pancreas; st, stomach. Scale bar: 100 µm.

(Fig. 1E,F). At E12.5, the ectopic pancreas tissue was typically found as a series of discrete patches along the dorsal stomach (Fig. 1G,H). However, in extreme cases, we noted ectopic pancreas tissue running anteriorly along the oesophagus and reaching the level of the oesophagotracheal septum anteriorly (Fig. S3). Thus, ectopic pancreas tissue is progressively found at more rostral locations as development proceeds. The penetrance of the ectopic pancreas phenotype in *Hes1*$^{-/-}$ embryos was 100% at all stages examined (>30 embryos in total), whereas it was never seen in wild types (>50 embryos in total).

To get a more detailed view of the boundary between the stomach and ectopic pancreas epithelia, we analysed transverse sections of the posterior foregut region by IF. At E10.5, the epithelium of the prospective forestomach expresses E-cadherin and encircles a simple lumen (Fig. 2B). This structure was preserved in *Hes1*$^{-/-}$ embryos, except that the dorsal part of the stomach epithelium was connected to an ectopic E-cadherin^{+} epithelium that extended in a dorsal direction (Fig. 2H). The ectopic dorsal epithelium contained Pdx1^{Hi}, Nkx6-1^{+} and glucagon^{+} cells, all markers of a pancreas fate, and was devoid of Sox2^{+} cells, which otherwise were found in the stomach epithelium proper in both *Hes1*$^{+/+}$ and *Hes1*$^{-/-}$ embryos (Fig. 2C-E,I-K). Pancreatic markers were absent at the level of prospective forestomach in wild types (Fig. 2C,D), while Nkx6-1 was found in ventral stomach mesenchyme (Fig. 2C,I) and Pdx1 in the ventral part of the posterior stomach epithelium (Fig. 2E,K), in both wild types and mutants.

Hes1 is required in the endoderm to prevent ectopic pancreas development

Specification of the dorsal pancreas from posterior foregut endoderm is dependent on signals from the notochord (Kim et al., 1997) and the vascular endothelium (Lammert et al., 2001; Yoshitomi and Zaret, 2004). Because *Hes1* is expressed in both the endoderm and the inducing tissues (Klinck et al., 2011), the ectopic pancreas phenotype could be the result of loss of Hes1 in either of these tissues. To distinguish between these possibilities, we conditionally deleted *Hes1* using Cre lines that are active in different combinations of these tissues. *Foxa2*-2A-iCre and *Sox17*-2A-iCre both delete efficiently in definitive endoderm but are also active outside the endoderm (Fig. 3A-C). However, the nonendodermal domains do not overlap between these two genes, so while *Foxa2*-2A-iCre is also active in the node, notochord and floor plate (Fig. 3B) (Horn et al., 2012), *Sox17*-2A-iCre is additionally active in vascular progenitor cells (Fig. 3C) (Engert et al., 2009). Accordingly, we generated *Hes1*$^{f/-}$; *Foxa2*$^{2A\text{-}iCre/+}$ (*Hes1*$^{\Delta Foxa2}$) and *Hes1*$^{f/-}$; *Sox17*$^{2A\text{-}iCre/+}$ (*Hes1*$^{\Delta Sox17}$) embryos and analysed the appearance of the posterior foregut region by whole-mount IF. E9.5 *Hes1*$^{\Delta Foxa2}$ and *Hes1*$^{\Delta Sox17}$ embryos both presented the anterior and posterior extensions of the Pdx1^{Hi} domain also seen in *Hes1*$^{-/-}$ embryos (Fig. 3D-F, compare with Fig. 1B). At E10.5, *Hes1*$^{\Delta Foxa2}$ and *Hes1*$^{\Delta Sox17}$ embryos both displayed pancreatic tissue along the entire dorsal aspect of the stomach in a manner indistinguishable from that observed in *Hes1*$^{-/-}$ embryos (Fig. 3G-I, compare with Fig. 1D). E12.5 *Hes1*$^{\Delta Foxa2}$ and *Hes1*$^{\Delta Sox17}$ embryos both had hypoplasia of the pancreas proper and ectopic pancreas tissue located in the dorsal part of the stomach as seen in *Hes1*$^{-/-}$ embryos (Fig. 3J-L, compare with Fig. 1H). The penetrance of the ectopic pancreas phenotype was 100% at all stages examined (18 embryos in total for the two conditional mutants). Together, these results indicate that Hes1 is required specifically in the endoderm, the only tissue in which both Cre lines are active.

Anterior ectopic pancreas tissue is derived from the dorsal pancreas anlage

We next wanted to determine the origin of the ectopic pancreas tissue. We considered two possibilities: first, it is possible that Hes1-deficient dorsal endoderm responds abnormally to inductive signals, e.g. from the notochord, resulting in the re-specification of prospective dorsal stomach endoderm into pancreas; second, it is possible that Hes1-deficient dorsal pancreas epithelium extends parallel to the gut tube, along the dorsal stomach endoderm, instead of extending perpendicularly to the gut tube, into its associated mesenchyme, as seen in wild types. To examine which of these alternative, but not necessarily mutually exclusive, possibilities contributes to ectopic pancreas formation, we performed lineage tracing with *Sox9*-CreER^{T2} and R26R-YFP mice (Kopp et al., 2011; Srinivas et al., 2001) on a *Hes1*$^{+/+}$ or *Hes1*$^{-/-}$ background (Fig. 4A). As shown above, Sox9 expression is confined to the dorsal pancreas anlage in both wild-type and *Hes1*$^{-/-}$ embryos (Fig. S1) at E8.0-E8.5, but soon thereafter it expands into the ventral pancreas as well as the endoderm of the prospective duodenum and stomach (Shih et al., 2015). Accordingly, 4-hydroxytamoxifen (4-OHT) administration at E9.5 resulted in embryos that showed extensive labelling of both ventral and dorsal pancreas, as well as stomach and intestine at E10.5 (Fig. S4A-C). Such embryos are

Development (2018) 145, dev163568. doi:10.1242/dev.163568

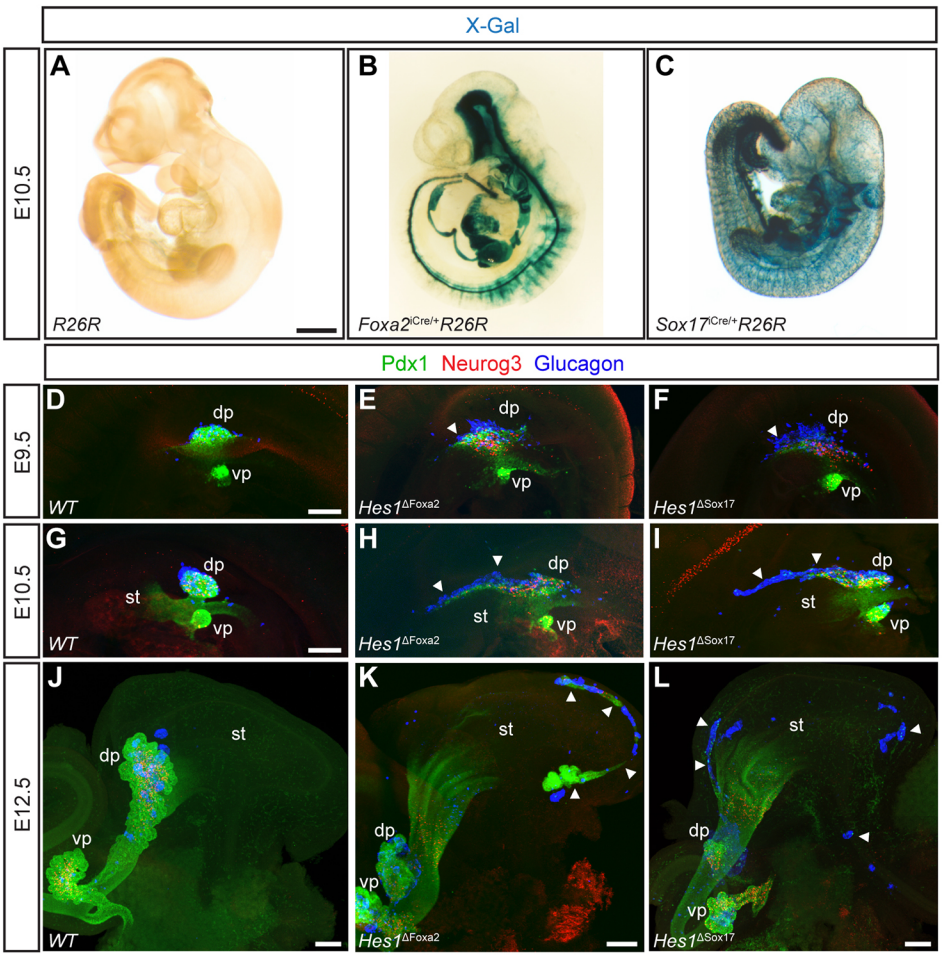

Fig. 3. Endodermal loss of Hes1 causes ectopic pancreas. (A-C) X-gal staining of *lacZ* activity in E10.5 embryos from crosses between *Rosa26R* and the two endodermal Cre-expressing lines *Foxa2*-2A-iCre and *Sox17*-2A-iCre, showing a wild-type control (A), *Foxa2*$^{iCre/+}$*R26*$^{lacZ/+}$ (B) and *Sox17*$^{iCre/+}$*R26*$^{lacZ/+}$(C). Projections of E9.5 (D-F), E10.5 (G-I) and E12.5 (J-L) pancreatic primordia from *Hes1*$^{+/+}$ (D,G,J), *Hes1*$^{\Delta Foxa2}$ (E,H,K) and *Hes1*$^{\Delta Sox17}$ (F,I,L) embryos, showing Pdx1, Neurog3 and glucagon by whole-mount IF. Arrowheads in E, F, H and I indicate the anterior extension of the dorsal pancreas in *Hes1*$^{\Delta Foxa2}$ and *Hes1*$^{\Delta Sox17}$ embryos. Arrowheads in K and L indicate patches of ectopic pancreas tissue located along the dorsal part of the stomach. dp, dorsal pancreas; st, stomach; vp, ventral pancreas. Scale bars: 100 µm.

uninformative for our purpose and were not pursued further. We therefore administered 4-OHT at E8.5 and quantified the number of labelled cells in the different midgut regions at E10.5 (Fig. 4A-D). On average, 94.8±7.0% (n=5) of the total YFP$^+$ cells were found in the dorsoanterior ectopic pancreas of *Hes1* mutants, which was similar to the 91.2±5.1% (mean±s.d., n=6) of the total YFP$^+$ cells found in the dorsal pancreas of controls (P=0.39). Correspondingly, no difference was seen between controls and mutants in the stomach (0.5±1.2% vs 2.2±3.6% YFP$^+$ cells, P=0.36) or intestine (8.0±5.9% vs 1.9±3.7% YFP$^+$ cells, P=0.10). Notably, the majority of the embryos in both groups showed no stomach labelling at all (Fig. 4D). Enlarged views of individual optical sections, focused on regions in which the ectopic pancreas tissue was juxtaposed to, or fused with, the dorsal stomach epithelium, revealed that labelled cells were confined to the ectopic pancreas tissue (Fig. S4D-N). These results demonstrate that at least part of the ectopic pancreas tissue found in stomach and oesophageal regions of *Hes1*$^{-/-}$ embryos is derived from an outwardly normal E8.5 dorsal pancreas primordium that subsequently undergoes a dysmorphic development. Nevertheless, these results do not refute that transdifferentiation of *Hes1*-deficient endoderm, induced by signals from dorsal mesoderm, might contribute to the ectopic pancreas tissue.

We therefore next explanted E9.5 *Hes1*$^{+/+}$*Pdx1*-GFP and *Hes1*$^{-/-}$*Pdx1*-GFP midguts and performed time-lapse imaging of the GFP signal to directly visualize dorsal bud formation. As can be seen in Movies 1 and 2, the dorsal buds of *Hes1*$^{+/+}$ and *Hes1*$^{+/-}$ explants display a relatively normal growth pattern, with the buds expanding in a dorsal direction with no extension along the rostrocaudal axis. In contrast, the dorsal bud of the *Hes1*$^{-/-}$ mutant fails to expand dorsally, but instead initiates a clear rostral extension (Movie 3). Moreover, no ectopic GFP signal appears in the stomach region of *Hes1*$^{-/-}$ explants. These data support the notion of aberrant morphogenesis as the cause of ectopic pancreas formation in *Hes1* mutants and argue against a cell-autonomous induction of transdifferentiation of stomach epithelium caused by loss of Hes1.

Dorsal pancreas dysgenesis and ectopic pancreas is Neurog3 dependent

To begin to understand the mechanism underlying ectopic pancreas formation we sought to identify changes in gene expression in Hes1-deficient pancreas cells. We therefore performed RNA sequencing (RNA-seq) on fluorescence-activated cell sorted (FACS) GFP$^+$ cells from individual E10.5 *Pdx1*-GFP; *Hes1*$^{+/+}$ (n=7) or *Pdx1*-GFP; *Hes1*$^{-/-}$ (n=4) embryos. Differential expression analysis revealed 75 upregulated and 47 downregulated genes [false discovery rate (FDR)-adjusted P<0.1] in the *Hes1*$^{-/-}$ compared with *Hes1*$^{+/+}$ embryos. As expected, many of the top upregulated transcripts, including *Arx*, *Cacna2d1*, *Cbfa2t3*, *Cck*, *Chga*, *Chgb*, *Cpe*, *Fbxl16*, *Fev*, *Gadd45a*, *Gfra3*, *Ghrl*, *Hmgn3*, *Ids*, *Lrp11*, *Neurod1*, *Neurog3*, *Pax6*, *Pclo*, *Pcsk1*, *Rab15*, *Slc38a5*, *Tmem27* (*Cltrn* – Mouse Genome Informatics) and *Upp1*, are enriched in endocrine cells and/or their precursors (Fig. 5A) (de Lichtenberg et al., 2018). Conversely, the top downregulated transcripts, which included – in addition to *Hes1* – *Adamts1*, *Chst2*, *Cpa1*, *Gc*, *Jag1*, *Matn4*, *Myc*, *Nr5a2* and *Wnt7b*, are enriched in

Development (2018) 145, dev163568. doi:10.1242/dev.163568

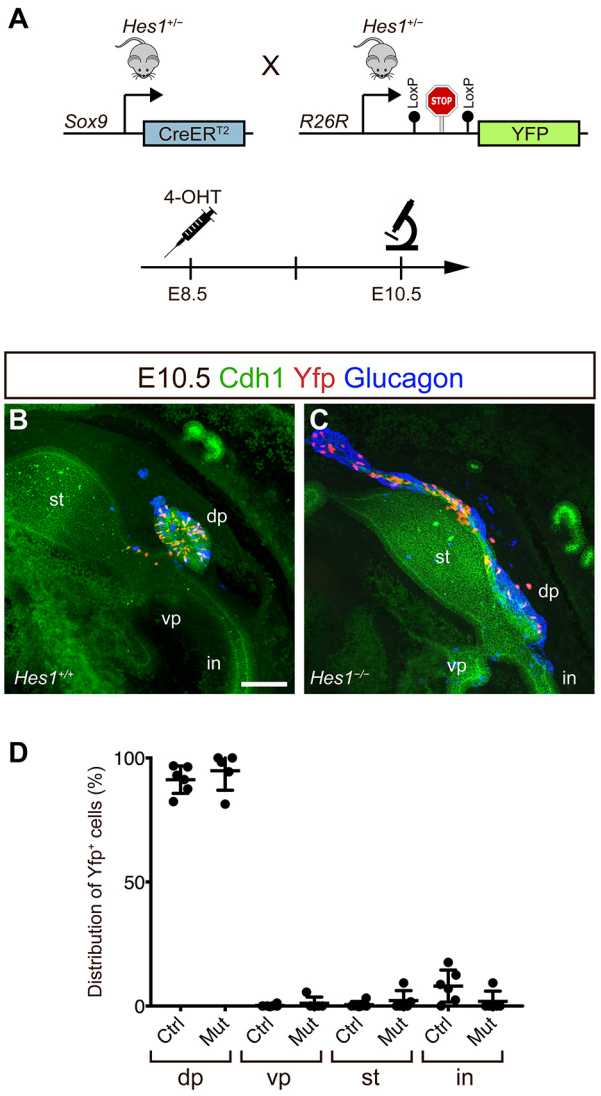

Fig. 4. Ectopic pancreas tissue is derived from the dorsal pancreas. (A) Schematic of the experimental setup. (B,C) Projections of E10.5 pancreatic primordia from *Sox9*-CreER^{T2}*R26R*$^{Yfp/+}$*Hes1*$^{+/+}$ (B) and *Sox9*-Cre^{ERT2}*R26R*$^{Yfp/+}$*Hes1*$^{-/-}$ (C) embryos from dams treated with 4-OHT at E8.5 and showing Cdh1, Yfp and glucagon by whole-mount IF. (D) Quantification of the distribution of labelled cells in the indicated midgut regions. *n*=6 for controls and *n*=5 for mutants; no *P*-values were significant (>0.05). Error bars indicate s.d. dp, dorsal pancreas; in, intestine; st, stomach; vp, ventral pancreas. Scale bar: 100 µm.

progenitor cells (Fig. 5A). Accordingly, the most significant gene ontology (GO) term for the upregulated genes is 'Endocrine systems development' (*P*=0.00004), but other significant terms, most notably 'Cell migration' (*P*=0.004) were also found high on the list. Among the genes associated with this GO term were many classical endocrine markers – *Chga*, *Arx*, *Pax6*, *Cck* and *Lhx1* – but also genes encoding GDNF receptor alpha 3 (*Gfra3*) and podocalyxin-like (*Podxl*), which have been associated with enhanced migration and invasion of non-small cell lung carcinoma cells and invasiveness in pancreatic cancer, respectively (Tang et al., 2010; Taniuchi et al., 2016). We therefore performed IF for these markers to uncover any potential correlation between these proteins and the ectopic pancreas phenotype. However, as shown in Fig. S5, Gfra3 was largely confined to endocrine cells as previously noted (Nivlet et al., 2016), and no difference between *Hes1*$^{-/-}$ and controls was observed. Podocalyxin-like was found at the apical side of most epithelial cells, wherever a microlumen had formed, but again without a noticeable difference between *Hes1*$^{-/-}$ and controls.

Thus, the RNA-seq data largely identified genes that were expected from the excessive endocrine differentiation known to occur in *Hes1* mutants.

Accordingly, we decided to directly test whether the endocrinogenic phenotype could be causally related to the dysmorphic development of the dorsal bud. We therefore generated *Hes1*$^{-/-}$*Neurog3*$^{-/-}$ double mutants with the aim of preventing endocrine differentiation (Gradwohl et al., 2000). As expected, the dorsal bud of E10.5 *Hes1*$^{-/-}$*Neurog3*$^{+/+}$ embryos from these crosses was dysmorphic, and Pdx1^{+}Ptf1a^{+} progenitors, as well as glucagon^{+} endocrine cells, extended along the entire dorsal part of the stomach compared with wild-type controls (Fig. 5B,C). Remarkably, the dorsal bud of *Hes1*$^{-/-}$*Neurog3*$^{-/-}$ embryos displayed the typical spherical appearance, albeit without signs of endocrine differentiation, comparable to *Neurog3*$^{-/-}$ embryos (Fig. 5D,E). Consistently, the prominent patches of ectopic pancreas along the stomach and oesophagus typically seen in E12.5 *Hes1*$^{-/-}$ embryos were absent from E12.5 *Hes1*$^{-/-}$*Neurog3*$^{-/-}$ embryos, although a few scattered glucagon^{+} cells could be found in both stomach and pancreatic regions (Fig. 5F-I). The appearance of these cells is remarkable in light of the lack of Neurog3, but is not without precedent. Scattered glucagon^{+} cells have previously been found in *Dll1*$^{-/-}$*Neurog3*$^{-/-}$ embryos (Ahnfelt-Rønne et al., 2012) and in certain *Neurog3*$^{-/-}$ strains (Wang et al., 2008). Nevertheless, these results demonstrate that the anterior extension of the dorsal pancreas at E10.5, and the resulting formation of ectopic pancreas tissue, depends on at least a part of the endocrine differentiation programme.

The strength of the endocrinogenic phenotype affects dorsal bud morphogenesis

Ectopic pancreas has so far not been described in mice with mutations in other Notch pathway genes, but not all have been analysed by methods that allow visualizing the GI tract in whole embryos. We therefore examined the appearance of the pancreatic buds in *Dll1*$^{\Delta Foxa2}$ and *Mib1*$^{\Delta Foxa2}$ embryos, as mutations in these two genes cause a weaker and stronger endocrinogenic phenotype, respectively (Ahnfelt-Rønne et al., 2012; Horn et al., 2012), compared with *Hes1*$^{-/-}$ and *Hes1*$^{\Delta Foxa2}$ (Fig. 6A-O). E9.5 dorsal buds showed some excessive endocrine differentiation in *Dll1*$^{\Delta Foxa2}$ and *Mib1*$^{\Delta Foxa2}$ embryos, but the MPC epithelium appeared relatively normal in morphology (Fig. 6A-C,G-I). E10.5 ventral buds were all relatively normal in appearance in these mutants, but the dorsal buds showed a distinctly different appearance, depending on which gene was mutated. *Dll1*$^{\Delta Foxa2}$ embryos displayed a hypoplastic, but otherwise well-formed, spherical bud with a cap of glucagon^{+} cells, no sign of an anterior extension and hypoplasia at E12.5, which is identical to that seen in *Dll1*$^{-/-}$ embryos (Fig. 6E,K,N) (Ahnfelt-Rønne et al., 2012; Horn et al., 2012). Remarkably, the dorsal bud of *Mib1*$^{\Delta Foxa2}$ embryos was severely hypoplastic, with the bud appearing completely converted into anteriorly extending glucagon^{+} cells (Fig. 6F,L). However, in contrast to *Hes1*$^{\Delta Foxa2}$ embryos, no ectopic pancreas is evident in E12.5 *Mib1*$^{\Delta Foxa2}$ embryos, although both dorsal and ventral buds are hypoplastic (Fig. 6M,O). These results show that the weak endocrinogenic phenotype of *Dll1* mutants correlates with a relatively normal dorsal bud morphogenesis, whereas the 'hyperendocrinogenic' *Mib1* mutant phenotype is associated with

Development (2018) 145, dev163568. doi:10.1242/dev.163568

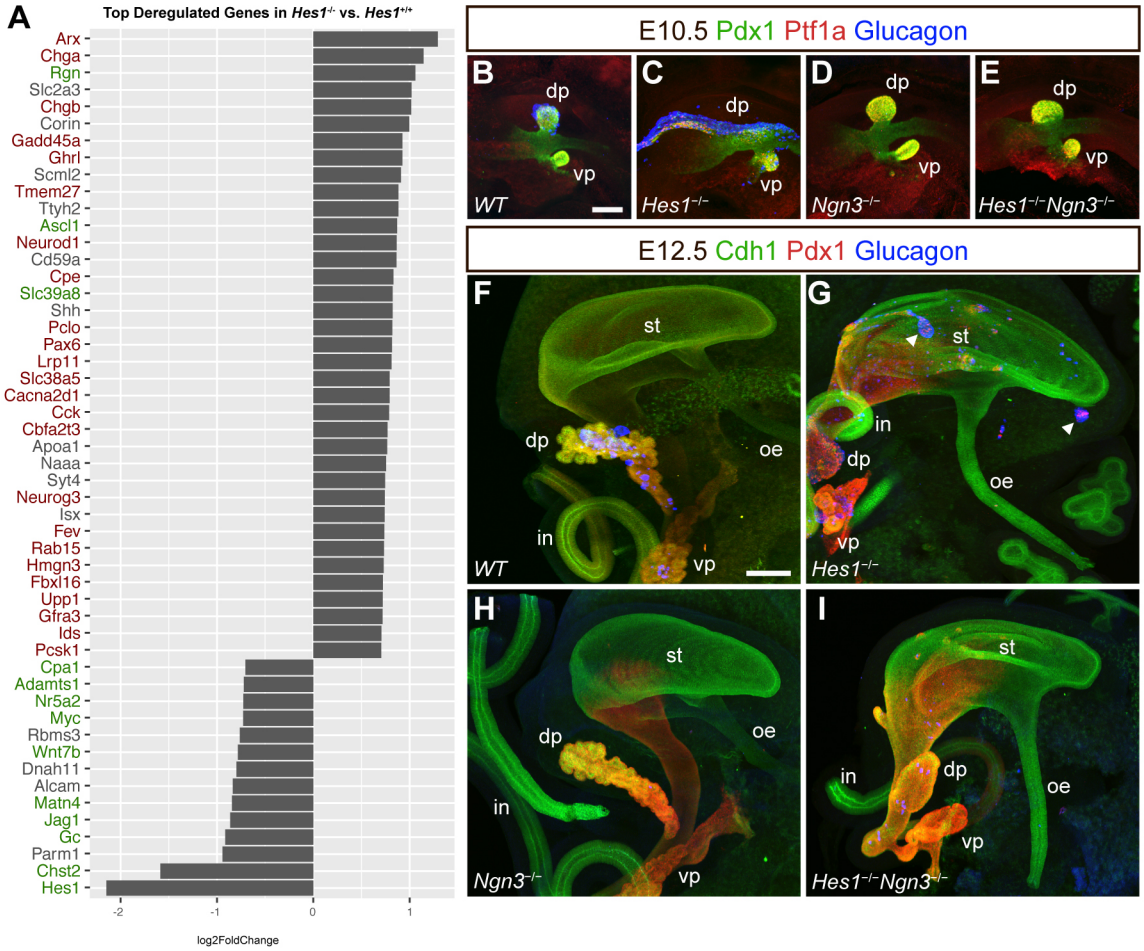

Fig. 5. Dysgenesis of the dorsal pancreas depends on *Neurog3*. (A) Differential expression analysis of sorted GFP$^+$ cells from individual *Pdx1*-GFP*; Hes1*$^{+/+}$ (*n*=7) and *Pdx1*-GFP*; Hes1*$^{-/-}$ (*n*=4) embryos, showing the top deregulated genes. Genes indicated in red are enriched in E15.5 endocrine lineage cells; genes indicated in green are enriched in E15.5 progenitors. (B-I) Maximum intensity projections of E10.5 (B-E) and E12.5 (F-I) midgut regions from *Hes1*$^{+/+}$*Neurog3*$^{+/+}$ (wild-type) (B,F), *Hes1*$^{-/-}$ (C,G), *Neurog3*$^{-/-}$ (D,H) and *Hes1*$^{-/-}$*Neurog3*$^{-/-}$ (E,I) embryos, showing Pdx1, Ptf1a and glucagon (B-E) or Cdh1, Pdx1 and glucagon (F-I) by whole-mount IF. Arrowheads indicate ectopic pancreas tissue. dp, dorsal pancreas; in, intestine; oe, oesophagus; st, stomach; vp, ventral pancreas. Scale bars: 100 µm.

an anteriorly extended, 'dorsal bud'-like endocrine structure, entirely depleted of progenitor cells, that eventually results in dorsal pancreas agenesis (Horn et al., 2012). These phenotypes contrast the overt ectopic pancreas phenotype seen in *Hes1* mutants (Fig. 6P).

DISCUSSION

Here, we show that the Notch signalling effector Hes1 is crucial for normal morphogenesis of the dorsal pancreas through its repression of Neurog3 and, at least partly, the endocrine differentiation program. In the absence of Hes1, the dorsal pancreas anlage fails to form the stalk during outgrowth from the gut tube and undergoes aberrant morphogenesis, initially leading to an anterior displacement of most of the dorsal pancreas epithelium to a position along the dorsal stomach epithelium. Parts of these two epithelia, both of which express E-cadherin, often appear merged at E10.5, suggesting that the anteriorly dislocated pancreas epithelium fuses with the dorsal stomach epithelium. Between E10.5 and E12.5, the stomach undergoes extensive morphogenetic transformation from an initially almost linear tube to a complex structure, in which the oesophagus moves towards the ventral side concomitant with a massive expansion of the dorsal part of the organ. We speculate that the initially contiguous cord of ectopic pancreas tissue seen at E10.5-E11.5 cannot expand as fast as the dorsal stomach, when the latter undergoes its major expansion between E11.5 and E12.5. Thus, the ectopic pancreas epithelium, which is likely adhering to the stomach endoderm through E-cadherin interactions, gets shredded, and this results in the formation of discrete patches of pancreatic tissue located adjacent to the dorsal stomach epithelium. However, in extreme cases, the anteriorly dislocated pancreatic tissue can reach an even more anterior position along the oesophagus.

Hes1 is considered to regulate endocrine differentiation by directly suppressing *Neurog3* expression in the endoderm; however, *Hes1* is also expressed in adjacent tissues, such as notochord and vascular endothelium (Klinck et al., 2011), that provide signals to the endoderm that are crucial for dorsal pancreas development (Kim et al., 1997; Lammert et al., 2001; Yoshitomi and Zaret, 2004). Thus, in spite of the notion that Hes1 acts in endoderm to regulate endocrine differentiation, the formation of ectopic pancreas tissue could be the result of loss of Hes1 in any of these tissues. Our finding that *Hes1*$^{\Delta Foxa2}$ embryos recapitulate the ectopic pancreas phenotype shows that Hes1 is required in *Foxa2*-expressing cells or their progeny, mainly the endoderm, node and notochord, and the

Development (2018) 145, dev163568. doi:10.1242/dev.163568

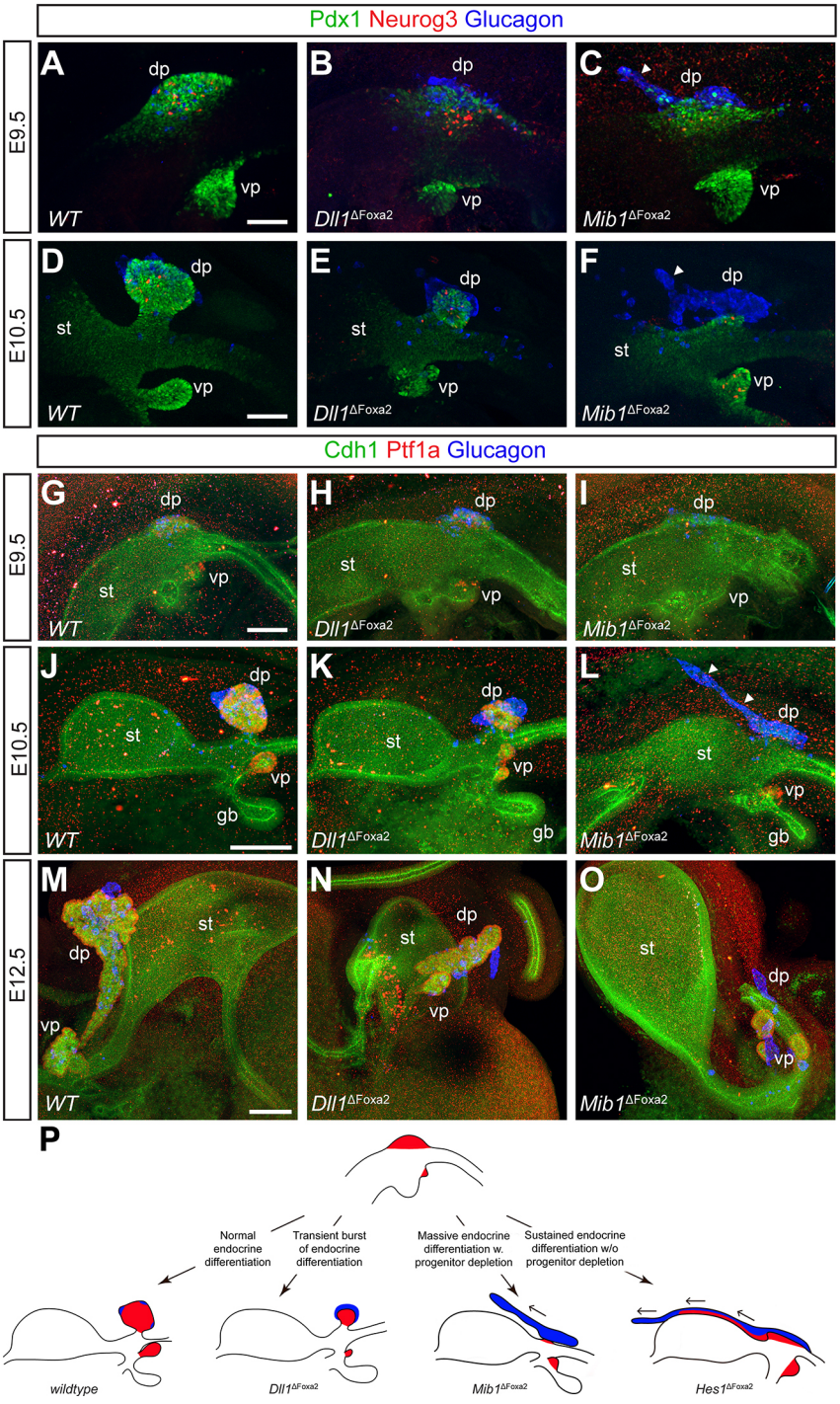

Fig. 6. Anterior extension of *Mib1* mutant glucagon cells. (A-O) Projections of E9.5 (A-C,G-I), E10.5 (D-F,J-L) and E12.5 (M-O) pancreatic primordia from *Hes1*$^{+/+}$ (A,D, G,J,M), *Dll1*$^{\Delta Foxa2}$ (B,E,H,K,N) and *Mib1*$^{\Delta Foxa2}$ (C,F,I,L,O) embryos, showing Pdx1, Neurog3 and glucagon (A-F) or Cdh1, Ptf1a and glucagon (G-O) by whole-mount IF. Arrowheads indicate anterior extension of glucagon cells in *Mib1*$^{\Delta Foxa2}$. (P) Schematic representation of pancreatic dysgenesis in different Notch pathway mutants. Red and blue indicate MPCs and endocrine cells, respectively. Compared with wild types, the dorsal buds of *Dll1* mutants show a short burst of excessive endocrinogenesis and reduced MPC proliferation (Ahnfelt-Rønne et al., 2012), resulting in a cap of glucagon^{+} cells surrounding a hypoplastic bud. The dorsal bud of *Mib1* mutants undergoes massive endocrinogenesis, leading to MPC depletion and, eventually, dorsal pancreas agenesis (Horn et al., 2012), by conversion to glucagon^{+} cells that migrate anteriorly (arrow). *Hes1* mutants undergo sustained and excessive endocrinogenesis without the near total progenitor depletion seen in *Mib1* mutants and ectopic tissue extends anteriorly along the stomach (arrows). dp, dorsal pancreas; gb, gall bladder; st, stomach; vp, ventral pancreas. Scale bars: 50 µm (A-F), 100 µm (G-O).

floor plate of the neural tube. Likewise, our finding that *Hes1*$^{\Delta Sox17}$ embryos recapitulate the ectopic pancreas phenotype shows that Hes1 is required in *Sox17*-expressing cells or their progeny, chiefly the endoderm and the vascular system. The most parsimonious explanation of these findings is that the loss of Hes1 in the endoderm is causing the formation of ectopic pancreas tissue. A mouse strain with strictly endoderm- or pancreas-specific Cre expression combined with highly efficient recombination prior to, or at the onset of, pancreas specification would have been the optimal choice to test this notion, but in spite of testing several lines we have not been able to secure a Cre deleter line that fulfils these requirements. Nevertheless, as discussed below, our finding that the additional deletion of *Neurog3* prevented the formation of ectopic pancreas tissue supports our conclusion regarding an endodermal requirement for Hes1.

The dorsoanterior location of the ectopic pancreas tissue analysed in this work suggests a couple of potential explanations for the underlying mechanism. Dorsal endoderm is patterned by the overlying notochord that, prior to embryo turning, is in direct contact with the dorsal midline endoderm along most of the rostrocaudal axis (Hebrok et al., 1998; Jørgensen et al., 2007; Kim et al., 1997). Nevertheless, only endoderm located at the pancreatic level responds to notochord signals by initiation of a pancreatic program (Hebrok et al., 1998; Kim et al., 1997). We first hypothesized

Development (2018) 145, dev163568. doi:10.1242/dev.163568

that the Hes1-deficient prospective dorsal stomach endoderm might acquire the competence to initiate a pancreatic program; for example, in response to notochord signals. However, our lineage-tracing experiment showed that Sox9^{+} cells located in the E8.5 dorsal pancreas primordium could contribute to the ectopic pancreas tissue without contributing to the stomach epithelium, which argues against transdifferentiation of stomach endoderm, at least as a pure cell-autonomous mechanism. Instead, these data support a model in which the morphogenesis of the dorsal pancreas bud is disturbed such that it extends parallel to the gut tube, along the dorsal stomach endoderm in *Hes1* mutants, rather than perpendicularly into its associated mesenchyme, as seen in wild types.

This finding appears to contradict the study of Fukuda and co-workers, who suggested that ectopic pancreas was caused by a transcommitment of the prospective stomach to pancreatic lineage by misexpression of *Ptf1a* (Fukuda et al., 2006). The authors of that study concluded that de-repression of *Ptf1a* in the absence of Hes1 was sufficient to induce this transcommitment. It should be noted though that the conclusion of Fukuda and co-workers was based primarily on two central observations. First, β-galactosidase labelling of ectopic pancreas tissue in *Hes1*$^{-/-}$*Ptf1a*$^{Cre/+}$; R26R animals. However, owing to its lack of time-dependent (i.e. tamoxifen-regulated) recombination, *Ptf1a*$^{Cre/+}$-based labelling does not allow one to distinguish ectopic, *de novo* expression of *Ptf1a* in stomach epithelium, from aberrant morphogenesis, resulting in *Ptf1a*-expressing pancreatic tissue being dislocated along the dorsal aspect of the stomach. Second, on transverse sections of stomach/ectopic pancreas tissue, Fukuda et al. found laminin immunoreactivity surrounding both tissues. This continuous basal lamina was interpreted as delamination of transdifferentiated ectopic pancreas tissue from the rest of the stomach. Yet, such a continuous basal lamina does not necessarily indicate a process of delamination. Instead, we propose that the dorsal pancreas tissue extends anteriorly between, or intercalating with, the stomach epithelium and the basal lamina in *Hes1* mutants, displacing the latter in a dorsal direction. However, even though we disagree with the interpretation, we think that the observations of Fukuda et al. are fully consistent with our proposal of aberrant morphogenesis causing ectopic pancreas. Conversely, we find it difficult to reconcile our observations with transdifferentiation of stomach endoderm. As mentioned above, our lineage-tracing data argue that transdifferentiation is not required for ectopic pancreas formation and the fact that concurrent deletion of *Neurog3* prevents ectopic pancreas formation in *Hes1* mutants is difficult to attribute to an effect exerted in the stomach epithelium, as *Neurog3* does not become expressed in main stomach epithelium until E12.5 in the *Hes1* mutants (E13.5 in wild types), two full days after overt ectopic pancreas formation is observed. If transdifferentiation of stomach endoderm, perhaps induced by signals from adjacent mesoderm, was occurring, one would expect that this would still occur in *Hes1*$^{-/-}$*Neurog3*$^{-/-}$ embryos.

Mutation of *Hes1* is the only mutation in the Notch pathway that, to date, has been observed to cause ectopic pancreas. Remarkably, when we examined pancreas development in *Mib1* mutants, the most prominent morphological feature of the E10.5 dorsal bud was an anterior extension reminiscent of that seen in *Hes1* mutants at the same stage. However, whereas this extension is composed of a mix of Pdx1^{+}Ptf1a^{+} progenitors and glucagon^{+} endocrine cells in the *Hes1* mutants, it is composed entirely of postmitotic glucagon^{+} cells in the *Mib1* mutants. In contrast, *Dll1* mutants, which display a rather weak endocrinogenic phenotype, displayed a hypoplastic, but otherwise well-formed spherical bud with a cap of glucagon^{+} cells and no sign of an anterior extension. Thus, the rather weak endocrinogenic phenotype of *Dll1* mutants, which declines before E9.5 (Ahnfelt-Rønne et al., 2012), allows for a relatively normal dorsal bud morphogenesis. In contrast, the stronger endocrinogenic phenotypes of *Hes1* and *Mib1* mutants are associated with a highly abnormal dorsal bud morphogenesis. However, the anteriorly extended dorsal bud of the 'hyperendocrinogenic' *Mib1* mutants is much less pronounced, perhaps because the extension in the *Mib1* mutant does not contain proliferating progenitor cells. We hypothesize that the disproportionate mix of Pdx1^{+}Ptf1a^{+} progenitors, Neurog3^{+} endocrine precursors and glucagon^{+} endocrine cells in the early dorsal pancreas of *Hes1* mutant embryos, perhaps in combination with loss of Hes1 in MPCs, provokes an aberrant morphogenesis, ultimately leading to ectopic pancreas (Fig. 6P). It would be interesting to test this notion by inducible expression of Neurog3 in either wild-type or e.g. *Dll1* mutant backgrounds.

Irrespective, the rescue of early dorsal bud morphogenesis seen in *Hes1*$^{-/-}$*Neurog3*$^{-/-}$ double-knockout embryos points to the endocrine cells and/or the Neurog3^{+} precursors as being involved in the formation of the anteriorly extended dorsal bud. One can imagine that excessive production of glucagon or PYY from the overabundant endocrine cells could affect cell motility. However, treatment of pregnant females with glucagon- and Y2-receptor antagonists yielded no evidence to suggest that these hormones played a role in the abnormal morphogenesis. Instead, we favour a hypothesis that it is the inherently motile phenotype of differentiating endocrine cells that is driving the anterior extension of the dorsal bud. When a vast excess of endocrine precursors and mature endocrine cells are delaminating from the epithelium, it is possible that they embark on an abnormal migratory route and that the disproportionality between endocrine lineage cells and MPCs makes it likely that the latter become dragged along in a passive process. Alternatively, the MPCs might contribute actively to the aberrant morphogenesis; for example, if their proliferation rate was increased. However, re-examination of our previously published confocal analysis of 5-bromo-2'-deoxyuridine (BrdU) incorporation (Ahnfelt-Rønne et al., 2012) showed that Pdx1^{+} cells in the E10.5 ectopic pancreas tissue had a marked reduction in BrdU incorporation compared with Pdx1^{+} dorsal bud cells from wild-type controls, arguing against this idea. However, it is noteworthy that the MPCs of the ectopic tissue are expected to maintain (or even increase) active Notch signalling in spite of (or due to) the loss of Hes1. Indeed, preliminary data indicate that such MPCs display strong expression of a BAC-transgenic *Hes1*-GFP reporter construct. Future experiments that conditionally inactivate genes required for motility of Neurog3^{+} cells or other Notch pathway genes could test these hypotheses.

Ectopic pancreas is occasionally found in humans and our results raise the possibility that *HES1* or other genes that affect *HES1* expression could be involved in the aetiology. Assuming that *HES1* function is conserved in humans, it is unlikely that global homozygosity for null alleles, i.e. through germ line transmission of *HES1* mutations, is involved, owing to the pleiotropic effects of global loss of *Hes1* (Ishibashi et al., 1995). However, somatic mutations, perhaps via loss of heterozygosity, could potentially lead to ectopic pancreas in humans. Genomic sequencing of resected ectopic pancreas tissue could help to resolve this issue.

MATERIALS AND METHODS

Animals and genotyping

The generation, breeding and genotyping of *Hes1*$^{+/-}$, *Hes1*$^{f/+}$, *Dll1*$^{f/+}$, *Mib1*$^{f/+}$, *Neurog3*^{tTA}, *Foxa2*^{T2AiCre}, *Sox17*^{T2AiCre}, *Sox9*-CreER^{T2}, *R26R*,

Development (2018) 145, dev163568. doi:10.1242/dev.163568

R26R-EYFP and *Pdx1*-GFP mouse lines have been reported previously (Engert et al., 2009; Horn et al., 2012; Imayoshi et al., 2008; Ishibashi et al., 1995; Koo et al., 2007; Kopp et al., 2011; Micallef et al., 2005; Soriano, 1999; Srinivas et al., 2001; Wang et al., 2009). Animals were maintained on a C57Bl/6J background. Littermate embryos were used as controls in all experiments. In lineage-tracing experiments, littermate *Hes1*$^{+/+}$*; Sox9*-CreER^{T2} mice were used as controls. Animals were maintained, and experiments were conducted, in adherence to guidelines issued by the European Convention for the Protection of Vertebrate Animals used for Experimental and other Scientific Purposes (ETS 123).

X-gal staining of *lacZ* activity

E10.5 embryos were dissected and fixed for 1 h in 0.2% glutaraldehyde/5 mM EGTA/100 mM $MgCl_2$/1× PBS. Embryos were washed for 3×5 min in 1× PBS and then incubated at 30°C overnight in 1 mg/ml X-gal (5-bromo-4-chloro-3-indolyl-β-D-galactopyranoside)/20 mM $K_3Fe(CN)_6$/20 mM $K_4Fe(CN)_6$*3H_2O/2 mM $MgCl_2$/0.01% NaDOC/0.02% Nonidet-P40/1× PBS. Embryos were washed for 3×5 min in 1× PBS and postfixed overnight at 4°C in 0.2% glutaraldehyde/1× PBS. Embryos were dehydrated stepwise in 1× PBS:MeOH (3:1, 2:2, 1:3) to 100% MeOH and cleared in BABB (1:2 benzyl alcohol:benzyl benzoate) before imaging.

Lineage tracing

Sox9-CreER^{T2}, *R26R*-EYFP and *Hes1*$^{+/-}$ animals were interbred to produce embryos carrying *Sox9*-CreER^{T2} and *R26R*-EYFP on *Hes1*$^{+/+}$ and *Hes1*$^{-/-}$ backgrounds. To label cells in the dorsal pancreas the pregnant females were injected intraperitoneally gestational days E8.5 and E9.5 with 0.05 mg/g body weight 4-OHT (Sigma-Aldrich, H6278) from a 10 mg/ml solution in corn oil (Sigma-Aldrich, C8267). Embryos were harvested at E10.5 and processed for whole-mount IF. From six litters, receiving 4-OHT at E8.5, we obtained seven *Sox9*-CreER^{T2+}*R26R*$^{Yfp/+}$*Hes1*$^{-/-}$ embryos that were analysed by whole-mount IF, together with a corresponding number of *Sox9*-CreER^{T2+}*R26R*$^{Yfp/+}$*Hes1*$^{+/+}$ and *Sox9*-CreER^{T2+}*R26R*$^{Yfp/+}$*Hes1*$^{+/-}$ littermate controls.

Statistical analysis

Statistical analysis was performed with two-tailed Student's *t*-test for unpaired samples. Sample size was determined post hoc. Three embryos with prominent labelling in ventral pancreas (≥18 YFP$^+$ cells) were excluded from the analysis. Embryos receiving 4-OHT at E9.5 showed extensive labelling of ventral and dorsal pancreas, as well as stomach and intestine at E10.5, and were not analysed further. The exclusion criteria were established post hoc.

Whole-mount IF

Embryos dissected at E10.5 and smaller stages were processed and stained as whole embryos, whereas at E11.5 and larger stages, the stomach-pancreas-duodenum block was dissected out. The tissue was fixed overnight at 4°C in 10% formalin in phosphate buffer, pH 7.2, washed for 3×30 min in 1× PBS, and then gently dehydrated stepwise in 1× PBS:MeOH (3:1, 2:2, 1:3) to 100% MeOH. The tissue was permeabilized for at least 2 h at room temperature (RT) in MeOH:DMSO:H_2O_2 (4:1:1) and then transferred back to 100% MeOH. The tissue was gently rehydrated in MeOH:1× PBS (3:1, 2:2, 1:3) to 1× PBS, blocked in 0.5% TNB (Perkin Elmer, NEL704A001KT)/1× PBS for 2 h at RT, and incubated with primary antibodies diluted in 0.5% TNB/1× PBS for 48 h at 4°C with gentle nutation. The tissue was washed 3× for 1 h in 1× PBS and incubated with Cy2-, Cy3- and Cy5-conjugated secondary antibodies raised in donkey (Jackson ImmunoResearch), diluted 1:500 in TNB/1× PBS for 48 h at 4°C with gentle nutation. For some of the rabbit antisera, a tyramide signal amplification (TSA) step was added to the protocol. Here, a biotinylated secondary antibody raised in donkey against rabbit IgG (Jackson ImmunoResearch) was applied together with the other secondary antibodies. After washing 3× for 1 h in 1× PBS, the tissue was incubated with peroxidase-conjugated streptavidin (PerkinElmer) for 48 h at 4°C with gentle nutation. The tissue was washed 3× for 1 h in 1× PBS and the signal developed with Cy3-TSA substrate, diluted 1:100 in amplification diluent (PerkinElmer) for 60-75 min at RT with gentle nutation and protected from light. The tissue was washed 3× for 1 h in 1× PBS, dehydrated stepwise in 1× PBS:MeOH (3:1, 2:2, 1:3) to 100% MeOH, and cleared in BABB before confocal imaging as described (Ahnfelt-Rønne et al., 2007).

Cryosectioning and IF

Embryos dissected at E10.5 were fixed overnight in 10% formalin in phosphate buffer, pH 7.2, washed 3× in 1× PBS and cryoprotected overnight in 30% sucrose/1× PBS. Embryos were then embedded in OCT (Sakura) and cryosectioned at 10 µm. Sections were rinsed in 1× PBS, blocked for 30 min in TNB/1× PBS, and incubated overnight with the primary antibodies diluted in TNB/1× PBS. Sections were washed for 3×5 min in 1× PBS and incubated for 30 min with A488-, Cy2-, Cy3- and Cy5-conjugated secondary antibodies raised in donkey (Jackson ImmunoResearch), diluted 1:500 in TNB/1× PBS. Sections were washed for 3×5 min in 1× PBS and mounted with 20% glycerol in 40 mM Tris base, pH 8.4. All steps in the staining procedure were performed at RT. Imaging was performed essentially as described in Klinck et al. (2011).

Primary antibodies

Primary antibodies used were as follows: goat anti-Foxa2 (Santa Cruz Biotechnology, sc-6554, 1:1000), rabbit anti-Nkx6-1 (Jensen et al., 1996) (1:500), goat anti-Pdx1 (BCBC, ab2027, 1:10,000), guinea pig anti-glucagon (Millipore, 4031-01F, 1:10,000), rabbit anti-GFP (Clontech, 632460, 1:2000, TSA), rabbit anti-Neurog3 (BCBC, ab2011, 1:10,000, TSA), rabbit anti-Ptf1a (BCBC, ab2153, 1:2000), rabbit anti-PYY (kind gift from Ole D. Madsen, 1:1000), rabbit anti-Sox2 (Chemicon, AB5603, 1:1000), rabbit anti-Sox9 (Millipore, AB5535, 1:1000), rat anti-Cdh1 (Novo Nordisk A/S, ECCD2, 1:2000), goat anti-Gfra3 (R&D Systems, AF2645, 1:500) and goat anti-Podxl (R&D Systems, AF1556, 1:500).

RNA-seq

Pdx1$^{GFP/+}$*; Hes1*$^{+/-}$ mice (Ishibashi et al., 1995; Micallef et al., 2005) were time mated with *Hes1*$^{+/-}$ mice and E10.5 embryos were isolated. The head and tail regions of each embryo were removed and used for genotyping. Each sample then consisted of the midbody, from the forelimb buds to the hindlimb buds. Based on previous cell sorting experiments, the total number of Pdx1$^+$ cells in the E10.5 pancreas is estimated to be 500-1000. To be able to sort out such a low number of GFP$^+$ cells, we were advised to spike the samples with a significant number of GFP$^-$ cells. As Pdx1, and Pdx1-GFP, is expressed strongly only in the pancreatic endoderm (GFP^{Hi} cells) and weaker in neighbouring duodenal and posterior stomach endoderm (GFP^{Lo} cells), we therefore did not dissect away nonpancreatic tissue, which is impossible to do in the mutant embryos anyway, but allowed this tissue to serve as a spike in each sample. We then used gating on the FACS to isolate GFP^{Hi} cells from GFP^{Lo} cells and GFP$^-$ cells. The samples were treated individually with Liberase TL (Roche) and DNAse I (Thermo Fisher Scientific) in Dulbecco's modified eagle medium (Thermo Fisher Scientific) for 20 min at 37°C, with shaking (1100 rpm) on a thermomixer to dissociate the cells, and subsequently spun down at 500 ***g*** for 5 min. The cells were suspended in 0.125% Trypsin-EDTA (Thermo Fisher Scientific) and, after 10 min at 37°C, the trypsinization was stopped with fetal bovine serum (FBS). Then, the cells were spun down at 500 ***g*** for 5 min and suspended in FACS buffer [2% FBS in PBS with 4′,6-diamidino-2-phenylindole (DAPI)]. Each embryo sample was sorted separately on a Sony SH800 cell sorter directly into RLT Plus (Qiagen). We retrieved 200-500 GFP$^+$ cells per embryo and RNA was purified with RNeasy Plus Micro (Qiagen) according to the manufacturer's instructions. RNA quality was verified using a Bioanalyser Pico Kit (Agilent) and the libraries were generated using the Ovation SoLo RNA-seq system (NuGen) according to the manufacturer's instructions. The libraries were quantified with Qubit high sensitivity DNA kit (Thermo Fisher Scientific) and sequenced with either HiSeq or NextSeq 500 sequencing systems (Illumina). The reads were mapped with STAR aligner (Dobin et al., 2013), and differential expression analysis between *Hes1*$^{+/+}$ and *Hes1*$^{-/-}$ samples was performed by DeSeq2 (Love et al., 2014), using independent filtering and an adjusted *P*-value of 0.1. GO term analysis was performed using PANTHER software (Mi et al., 2013); REVIGO software (Supek et al., 2011) was used to cluster GO terms in semantic space.

Development (2018) 145, dev163568. doi:10.1242/dev.163568

The RNA-seq data have been deposited to ArrayExpress under the accession number E-MTAB-6890.

Image analysis

All IF images were captured using point scanning confocal Zeiss Axioimager systems (LSM510, LSM700 and LSM710). *Z*-stacks and tiled *z*-stacks from whole-mount-IF-stained tissue were stitched and projected to 3D using Zeiss Zen software. Alignment of two images to produce the composite image in Fig. 1H was performed manually with Adobe Photoshop.

Live imaging

Eight-well culture slides with glass bottom (Ibidi, 80827) were coated with 1 µg/ml fibronectin (Sigma-Aldrich, F1141) in 100 mM NaCl the day before explant isolation and stored at 4°C. *Pdx1*$^{GFP/+}$*; Hes1*$^{+/-}$ mice were time mated with *Hes1*$^{+/-}$ mice and E9.5 embryos were isolated. The foregut/midgut region of the primitive gut tube containing prospective stomach, pancreas and duodenum was microdissected in ice-cold dissection medium [1× minimum essential medium (MEM) with Hank's Salts and L-glutamine (Gibco, 21575-022), 10% FBS, 50 µg/ml gentamicin (Gibco, 15750-037)] from each embryo. We observed that 17/37 isolated gut tubes expressed GFP in the pancreas primordium. The GFP$^+$ explants were placed left side down on the glass bottom of the culture wells in 37°C pre-warmed culture medium [1× MEM with Earle's Salts and L-glutamine (Gibco, 11095-080), 20% FBS, 50 µg/ml gentamicin (Gibco, 15750-037), 0.1 µg/ml FGF10 (R&D Systems, 6224-FG)]. The explants were allowed to attach overnight at 37°C before imaging. Live recordings of the Pdx1-GFP signal in dorsal pancreatic bud development were captured on a confocal Zeiss LSM880 with an Airyscan module using a Plan Apochromat 20×/0.80 NA objective (420650-9901-000). *Z*-stacks of 24 slices of 2 µm optical sections with minimal overlap were recorded every 20 min for 16 h, after which viability was affected in most explants. Movies were recorded in Imaris 9.0.2 software (Bitplane).

Acknowledgements

We thank Ryoichiro Kageyama for mice; Karsten Marckstrøm for technical assistance; Helen Neil, Gelo de la Cruz, Jutta Bulkescher, Gopal Karemore and the Center for Integrated Microscopy for help with cell sorting, RNA-seq, imaging and image data analysis; and Gerard Gradwohl, Phil Seymour and Thue W. Schwartz for advice.

Competing interests

The authors declare no competing or financial interests.

Author contributions

Conceptualization: M.C.J., P.S.; Methodology: M.C.J., K.H.d.L., J.H.E., M.S.E.; Formal analysis: M.C.J., R.K., P.S.; Investigation: M.C.J., K.H.d.L., C.A.C., R.K., J.H.E., M.S.E.; Resources: H.L.; Data curation: M.C.J.; Writing - original draft: M.C.J., K.H.d.L., P.S.; Writing - review & editing: M.C.J., K.H.d.L., H.L., P.S.; Visualization: M.C.J., C.A.C., R.K.; Supervision: P.S.; Project administration: M.C.J., P.S.; Funding acquisition: P.S.

Funding

Funding for this work was provided by Novo Nordisk Fonden [16076 and 10717] and the Juvenile Diabetes Research Foundation International [1-2009-309]. The Novo Nordisk Foundation Center for Stem Cell Biology is supported by Novo Nordisk Fonden [NNF17CC0027852].

Data availability

RNA-seq data are available at ArrayExpress under the accession number E-MTAB-6890.

Supplementary information

Supplementary information available online at
http://dev.biologists.org/lookup/doi/10.1242/dev.163568.supplemental

References

Afelik, S., Qu, X., Hasrouni, E., Bukys, M. A., Deering, T., Nieuwoudt, S., Rogers, W., Macdonald, R. J. and Jensen, J. (2012). Notch-mediated patterning and cell fate allocation of pancreatic progenitor cells. *Development* **139**, 1744-1753.

Ahlgren, U., Pfaff, S. L., Jessell, T. M., Edlund, T. and Edlund, H. (1997). Independent requirement for ISL1 in formation of pancreatic mesenchyme and islet cells. *Nature* **385**, 257-260.

Ahnfelt-Rønne, J., Jørgensen, M. C., Hald, J., Madsen, O. D., Serup, P. and Hecksher-Sørensen, J. (2007). An improved method for three-dimensional reconstruction of protein expression patterns in intact mouse and chicken embryos and organs. *J. Histochem. Cytochem.* **55**, 925-930.

Ahnfelt-Rønne, J., Jørgensen, M. C., Klinck, R., Jensen, J. N., Füchtbauer, E.-M., Deering, T., MacDonald, R. J., Wright, C. V. E., Madsen, O. D. and Serup, P. (2012). Ptf1a-mediated control of Dll1 reveals an alternative to the lateral inhibition mechanism. *Development* **139**, 33-45.

Apelqvist, A., Ahlgren, U. and Edlund, H. (1997). Sonic hedgehog directs specialised mesoderm differentiation in the intestine and pancreas. *Curr. Biol.* **7**, 801-804.

Apelqvist, A., Li, H., Sommer, L., Beatus, P., Anderson, D. J., Honjo, T., Hrabe de Angelis, M., Lendahl, U. and Edlund, H. (1999). Notch signalling controls pancreatic cell differentiation. *Nature* **400**, 877-881.

Bastidas-Ponce, A., Scheibner, K., Lickert, H. and Bakhti, M. (2017). Cellular and molecular mechanisms coordinating pancreas development. *Development* **144**, 2873-2888.

Bitgood, M. J. and McMahon, A. P. (1995). Hedgehog and Bmp genes are coexpressed at many diverse sites of cell-cell interaction in the mouse embryo. *Dev. Biol.* **172**, 126-138.

de Lichtenberg, K. H., Seymour, P. A., Jørgensen, M. C., Kim, Y.-H., Grapin-Botton, A., Magnuson, M., Nakic, N., Ferrer, J. and Serup, P. (2018). Notch controls multiple pancreatic cell fate regulators through direct Hes1-mediated repression. *bioRxiv*, 336305.

Dobin, A., Davis, C. A., Schlesinger, F., Drenkow, J., Zaleski, C., Jha, S., Batut, P., Chaisson, M. and Gingeras, T. R. (2013). STAR: ultrafast universal RNA-seq aligner. *Bioinformatics* **29**, 15-21.

Echelard, Y., Epstein, D. J., St-Jacques, B., Shen, L., Mohler, J., McMahon, J. A. and McMahon, A. P. (1993). Sonic hedgehog, a member of a family of putative signaling molecules, is implicated in the regulation of CNS polarity. *Cell* **75**, 1417-1430.

Engert, S., Liao, W. P., Burtscher, I. and Lickert, H. (2009). Sox17-2A-iCre: a knock-in mouse line expressing Cre recombinase in endoderm and vascular endothelial cells. *Genesis* **47**, 603-610.

Fujikura, J., Hosoda, K., Iwakura, H., Tomita, T., Noguchi, M., Masuzaki, H., Tanigaki, K., Yabe, D., Honjo, T. and Nakao, K. (2006). Notch/Rbp-j signaling prevents premature endocrine and ductal cell differentiation in the pancreas. *Cell Metab.* **3**, 59-65.

Fujikura, J., Hosoda, K., Kawaguchi, Y., Noguchi, M., Iwakura, H., Odori, S., Mori, E., Tomita, T., Hirata, M., Ebihara, K. et al. (2007). Rbp-j regulates expansion of pancreatic epithelial cells and their differentiation into exocrine cells during mouse development. *Dev. Dyn.* **236**, 2779-2791.

Fukuda, A., Kawaguchi, Y., Furuyama, K., Kodama, S., Horiguchi, M., Kuhara, T., Koizumi, M., Boyer, D. F., Fujimoto, K., Doi, R. et al. (2006). Ectopic pancreas formation in Hes1 -knockout mice reveals plasticity of endodermal progenitors of the gut, bile duct, and pancreas. *J. Clin. Invest.* **116**, 1484-1493.

Gradwohl, G., Dierich, A., LeMeur, M. and Guillemot, F. (2000). neurogenin3 is required for the development of the four endocrine cell lineages of the pancreas. *Proc. Natl. Acad. Sci. USA* **97**, 1607-1611.

Hald, J., Hjorth, J. P., German, M. S., Madsen, O. D., Serup, P. and Jensen, J. (2003). Activated Notch1 prevents differentiation of pancreatic acinar cells and attenuate endocrine development. *Dev. Biol.* **260**, 426-437.

Hebrok, M., Kim, S. K. and Melton, D. A. (1998). Notochord repression of endodermal Sonic hedgehog permits pancreas development. *Genes Dev.* **12**, 1705-1713.

Hebrok, M., Kim, S. K., St Jacques, B., McMahon, A. P. and Melton, D. A. (2000). Regulation of pancreas development by hedgehog signaling. *Development* **127**, 4905-4913.

Horn, S., Kobberup, S., Jorgensen, M. C., Kalisz, M., Klein, T., Kageyama, R., Gegg, M., Lickert, H., Lindner, J., Magnuson, M. A. et al. (2012). Mind bomb 1 is required for pancreatic beta-cell formation. *Proc. Natl. Acad. Sci. USA* **109**, 7356-7361.

Hörnblad, A., Eriksson, A. U., Sock, E., Hill, R. E. and Ahlgren, U. (2011). Impaired spleen formation perturbs morphogenesis of the gastric lobe of the pancreas. *PLoS ONE* **6**, e21753.

Imayoshi, I., Shimogori, T., Ohtsuka, T. and Kageyama, R. (2008). Hes genes and neurogenin regulate non-neural versus neural fate specification in the dorsal telencephalic midline. *Development* **135**, 2531-2541.

Ishibashi, M., Ang, S. L., Shiota, K., Nakanishi, S., Kageyama, R. and Guillemot, F. (1995). Targeted disruption of mammalian hairy and Enhancer of split homolog-1 (HES-1) leads to up-regulation of neural helix-loop-helix factors, premature neurogenesis, and severe neural tube defects. *Genes Dev.* **9**, 3136-3148.

Jensen, J., Serup, P., Karlsen, C., Nielsen, T. F. and Madsen, O. D. (1996). mRNA profiling of rat islet tumors reveals nkx 6.1 as a beta-cell-specific homeodomain transcription factor. *J. Biol. Chem.* **271**, 18749-18758.

Jensen, J., Pedersen, E. E., Galante, P., Hald, J., Heller, R. S., Ishibashi, M., Kageyama, R., Guillemot, F., Serup, P. and Madsen, O. D. (2000). Control of endodermal endocrine development by Hes-1. *Nat. Genet.* **24**, 36-44.

Jørgensen, M. C., Ahnfelt-Rønne, J., Hald, J., Madsen, O. D., Serup, P. and Hecksher-Sørensen, J. (2007). An illustrated review of early pancreas development in the mouse. *Endocr. Rev.* **28**, 685-705.
Kim, S. K., Hebrok, M. and Melton, D. A. (1997). Notochord to endoderm signaling is required for pancreas development. *Development* **124**, 4243-4252.
Klinck, R., Füchtbauer, E.-M., Ahnfelt-Rønne, J., Serup, P., Jensen, J. N. and Jørgensen, M. C. (2011). A BAC transgenic Hes1-EGFP reporter reveals novel expression domains in mouse embryos. *Gene Expr. Patterns* **11**, 415-426.
Koo, B.-K., Yoon, M.-J., Yoon, K.-J., Im, S.-K., Kim, Y.-Y., Kim, C.-H., Suh, P.-G., Jan, Y. N. and Kong, Y.-Y. (2007). An obligatory role of mind bomb-1 in notch signaling of mammalian development. *PLoS ONE* **2**, e1221.
Kopp, J. L., Dubois, C. L., Schaffer, A. E., Hao, E., Shih, H. P., Seymour, P. A., Ma, J. and Sander, M. (2011). Sox9+ ductal cells are multipotent progenitors throughout development but do not produce new endocrine cells in the normal or injured adult pancreas. *Development* **138**, 653-665.
Lammert, E., Cleaver, O. and Melton, D. (2001). Induction of pancreatic differentiation by signals from blood vessels. *Science* **294**, 564-567.
Love, M. I., Huber, W. and Anders, S. (2014). Moderated estimation of fold change and dispersion for RNA-seq data with DESeq2. *Genome Biol.* **15**, 550.
Mi, H., Muruganujan, A. and Thomas, P. D. (2013). PANTHER in 2013: modeling the evolution of gene function, and other gene attributes, in the context of phylogenetic trees. *Nucleic Acids Res.* **41**, D377-D386.
Micallef, S. J., Janes, M. E., Knezevic, K., Davis, R. P., Elefanty, A. G. and Stanley, E. G. (2005). Retinoic acid induces Pdx1-positive endoderm in differentiating mouse embryonic stem cells. *Diabetes* **54**, 301-305.
Murtaugh, L. C., Stanger, B. Z., Kwan, K. M. and Melton, D. A. (2003). Notch signaling controls multiple steps of pancreatic differentiation. *Proc. Natl. Acad. Sci. USA* **100**, 14920-14925.
Nivlet, L., Herrmann, J., Martin, D. E., Meunier, A., Orvain, C. and Gradwohl, G. (2016). Expression and functional studies of the GDNF family receptor alpha 3 in the pancreas. *J. Mol. Endocrinol.* **56**, 77-90.
Ramalho-Santos, M., Melton, D. A. and McMahon, A. P. (2000). Hedgehog signals regulate multiple aspects of gastrointestinal development. *Development* **127**, 2763-2772.
Schaffer, A. E., Freude, K. K., Nelson, S. B. and Sander, M. (2010). Nkx6 transcription factors and Ptf1a function as antagonistic lineage determinants in multipotent pancreatic progenitors. *Dev. Cell* **18**, 1022-1029.
Shih, H. P., Seymour, P. A., Patel, N. A., Xie, R., Wang, A., Liu, P. P., Yeo, G. W., Magnuson, M. A. and Sander, M. (2015). A gene regulatory network cooperatively controlled by Pdx1 and Sox9 governs lineage allocation of foregut progenitor cells. *Cell Rep.* **13**, 326-336.
Soriano, P. (1999). Generalized lacZ expression with the ROSA26 Cre reporter strain. *Nat. Genet.* **21**, 70-71.
Spence, J. R., Lange, A. W., Lin, S.-C. J., Kaestner, K. H., Lowy, A. M., Kim, I., Whitsett, J. A. and Wells, J. M. (2009). Sox17 regulates organ lineage segregation of ventral foregut progenitor cells. *Dev. Cell* **17**, 62-74.
Srinivas, S., Watanabe, T., Lin, C.-S., William, C. M., Tanabe, Y., Jessell, T. M. and Costantini, F. (2001). Cre reporter strains produced by targeted insertion of EYFP and ECFP into the ROSA26 locus. *BMC Dev. Biol.* **1**, 4.
Sumazaki, R., Shiojiri, N., Isoyama, S., Masu, M., Keino-Masu, K., Osawa, M., Nakauchi, H., Kageyama, R. and Matsui, A. (2004). Conversion of biliary system to pancreatic tissue in Hes1-deficient mice. *Nat. Genet.* **36**, 83-87.
Supek, F., Bošnjak, M., Škunca, N. and Šmuc, T. (2011). REVIGO summarizes and visualizes long lists of gene ontology terms. *PLoS ONE* **6**, e21800.
Tadokoro, H., Takase, M. and Nobukawa, B. (2011). Development and congenital anomalies of the pancreas. *Anat. Res. Int.* **2011**, 351217.
Tang, J.-Z., Kong, X.-J., Kang, J., Fielder, G. C., Steiner, M., Perry, J. K., Wu, Z.-S., Yin, Z., Zhu, T., Liu, D.-X. et al. (2010). Artemin-stimulated progression of human non-small cell lung carcinoma is mediated by BCL2. *Mol. Cancer Ther.* **9**, 1697-1708.
Taniuchi, K., Furihata, M., Naganuma, S., Dabanaka, K., Hanazaki, K. and Saibara, T. (2016). Podocalyxin-like protein, linked to poor prognosis of pancreatic cancers, promotes cell invasion by binding to gelsolin. *Cancer Sci.* **107**, 1430-1442.
Türkvatan, A., Erden, A., Türkoğlu, M. A. and Yener, O. (2013). Congenital variants and anomalies of the pancreas and pancreatic duct: imaging by magnetic resonance cholangiopancreaticography and multidetector computed tomography. *Korean J. Radiol.* **14**, 905-913.
Upchurch, B. H., Aponte, G. W. and Leiter, A. B. (1994). Expression of peptide YY in all four islet cell types in the developing mouse pancreas suggests a common peptide YY-producing progenitor. *Development* **120**, 245-252.
Villasenor, A., Chong, D. C., Henkemeyer, M. and Cleaver, O. (2010). Epithelial dynamics of pancreatic branching morphogenesis. *Development* **137**, 4295-4305.
Wang, S., Hecksher-Sorensen, J., Xu, Y., Zhao, A., Dor, Y., Rosenberg, L., Serup, P. and Gu, G. (2008). Myt1 and Ngn3 form a feed-forward expression loop to promote endocrine islet cell differentiation. *Dev. Biol.* **317**, 531-540.
Wang, S., Jensen, J. N., Seymour, P. A., Hsu, W., Dor, Y., Sander, M., Magnuson, M. A., Serup, P. and Gu, G. (2009). Sustained Neurog3 expression in hormone-expressing islet cells is required for endocrine maturation and function. *Proc. Natl. Acad. Sci. USA* **106**, 9715-9720.
Yoshitomi, H. and Zaret, K. S. (2004). Endothelial cell interactions initiate dorsal pancreas development by selectively inducing the transcription factor Ptf1a. *Development* **131**, 807-817.

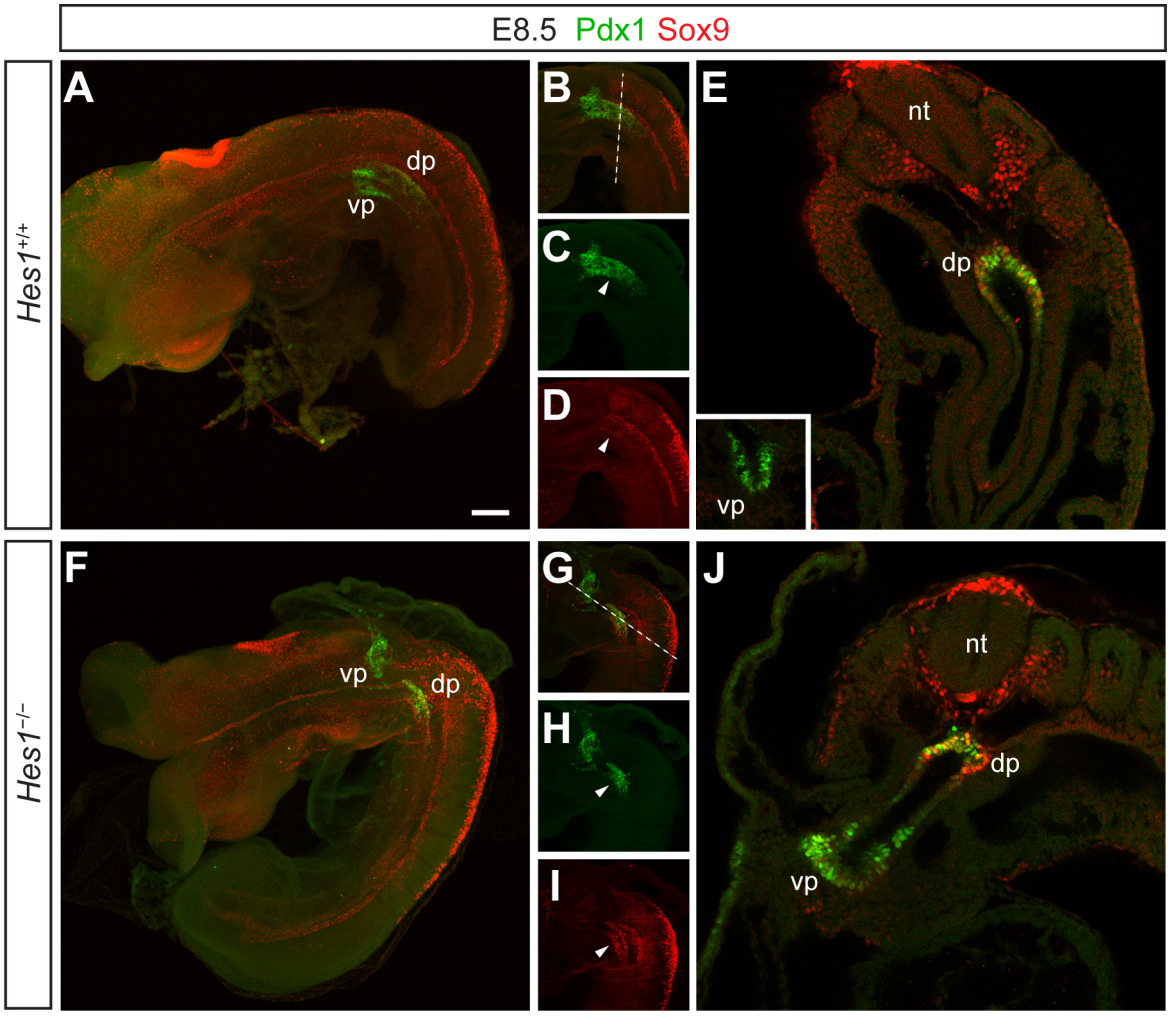

Fig. S1. The pancreas is specified normally in *Hes1* mutants. Projections of E8.5 *Hes1*$^{+/+}$ (A) and *Hes1*$^{-/-}$ (F) embryos showing Pdx1 and Sox9 by whole-mount IF. (B–D) Close-ups of *Hes1*$^{+/+}$ pancreatic anlage. (E) Optical section of embryo shown in (A) with the hatched line in (B) indicates the plane of the section. Insert shows ventral pancreas on a different optical section. (G–I) Close-ups of *Hes1*$^{-/-}$ pancreatic anlage. Note that early endodermal Sox9 expression is restricted to the dorsal pancreas anlage. The hatched line in (G) indicates the plane of the section shown in (*J*). dp: dorsal pancreas, vp: ventral pancreas, nt: neural tube. Scale bar is 100 µm.

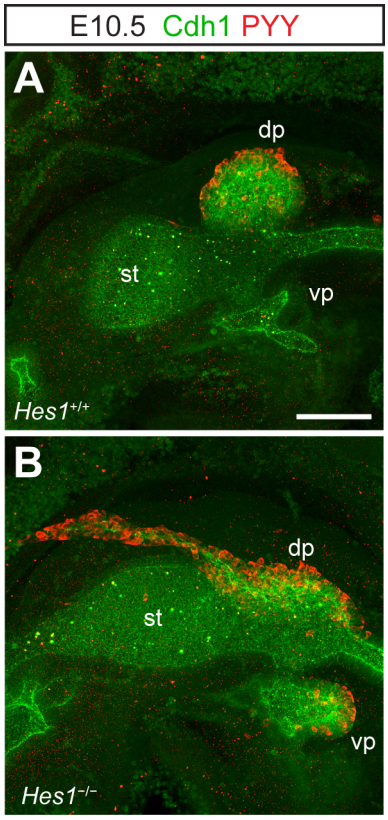

Fig. S2. PYY is expressed in the endocrine cells of *Hes1* mutants. E10.5 pancreatic primordia from *Hes1*$^{+/+}$ (A) and *Hes1*$^{-/-}$ (B) embryos showing Cdh1 and PYY by whole-mount IF. st: stomach, dp: dorsal pancreas, vp: ventral pancreas. Scale bar is 100 µm.

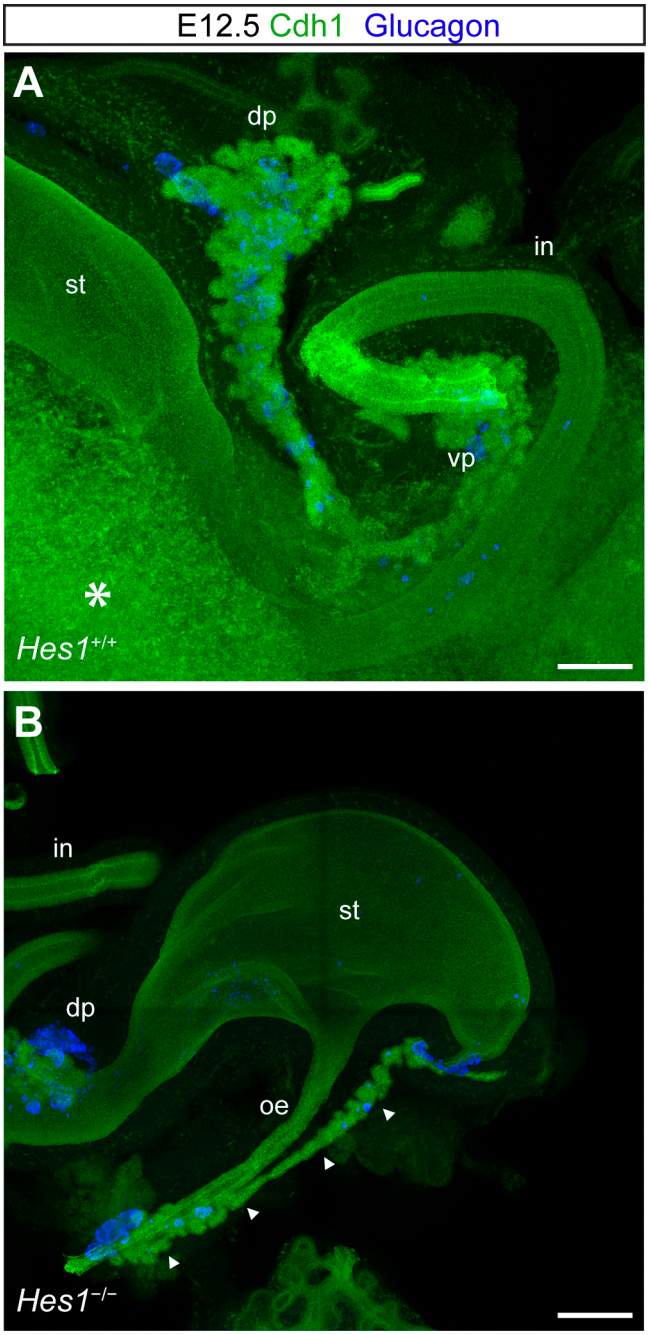

Fig. S3. Extreme anterior localization of ectopic pancreas. E12.5 *Hes1*$^{+/+}$ (A) and *Hes1*$^{-/-}$ (B) embryos showing Cdh1 and glucagon by whole-mount IF. (A) Asterisk indicates remaining liver. Scale bar is 100 µm. (B) Composite image created by automatic tiling of four individual confocal image stacks. Arrowheads indicate ectopic pancreas. st: stomach, dp: dorsal pancreas, oe: oesophagus, in: intestine. Scale bar is 200 µm.

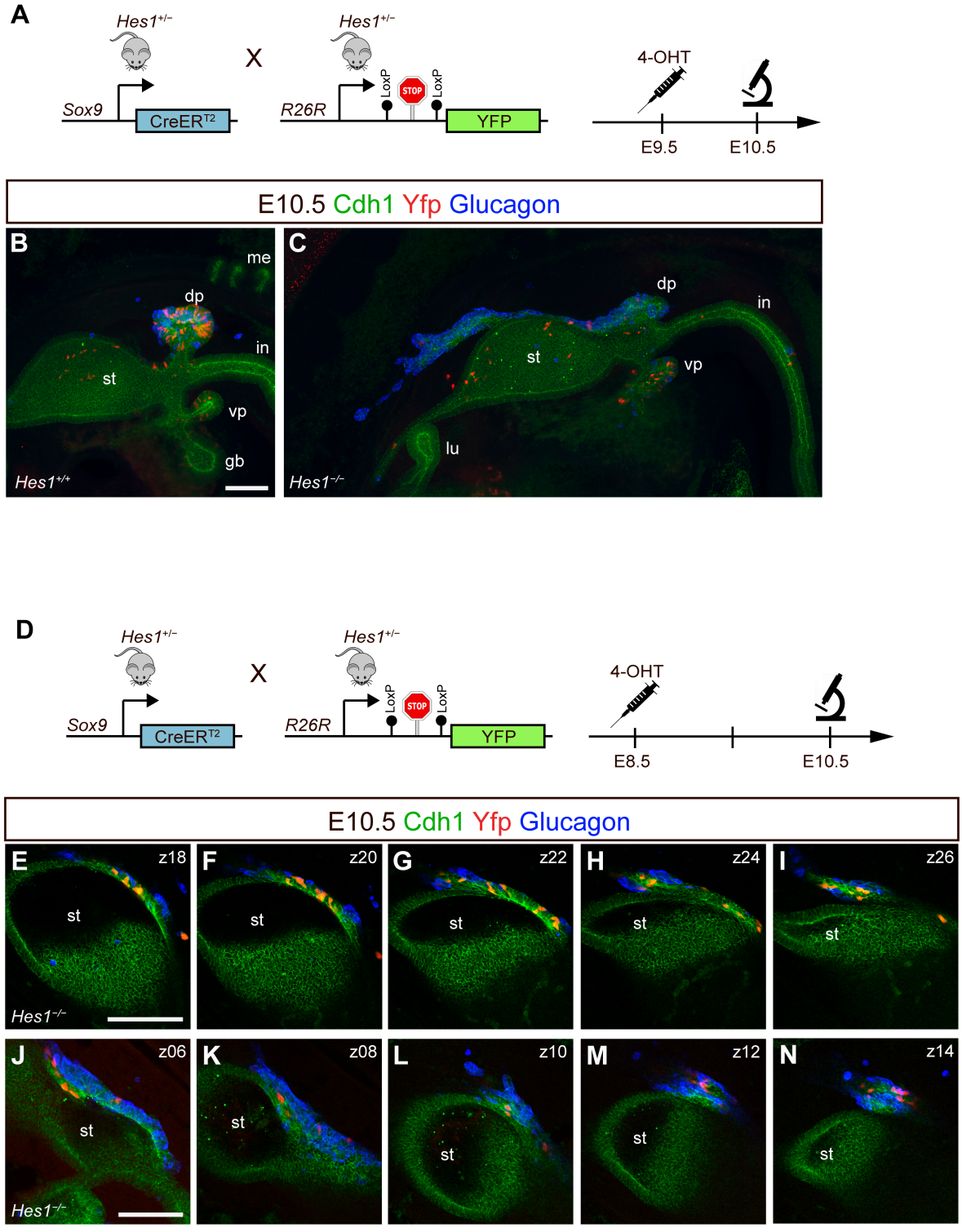

Fig. S4. Sox9-CreERT2 lineage tracing at E9.5 and E8.5. (A) Schematic of experimental setup with 4-OHT administration at E9.5. (B,C) Projections of E10.5 pancreatic primordia from *Sox9*-CreER^{T2}*R26R*$^{yfp/+}$*Hes1*$^{+/+}$ (B) and *Sox9*-CreER^{T2}*R26R*$^{yfp/+}$*Hes1*$^{-/-}$ (C) embryos from dams treated with 4-OHT at E9.5 and showing Cdh1, Yfp, and glucagon by whole-mount IF. Note that a significant number of the labeled cells reside outside the dorsal (ectopic) pancreas area. (D) Schematic of experimental setup with 4-OHT administration at E8.5. (E-N) Individual optical sections of two different *Sox9*-Cre^{ERT2}*R26R*$^{Yfp/+}$*Hes1*$^{-/-}$ embryos. The optical section (z) is indicated for each embryo (E-I and J-N, respectively). st: stomach, dp: dorsal pancreas, vp: ventral pancreas, in: intestine, lu: lung, gb: gall bladder, me: mesonephros. Scale bars are 100 µm.

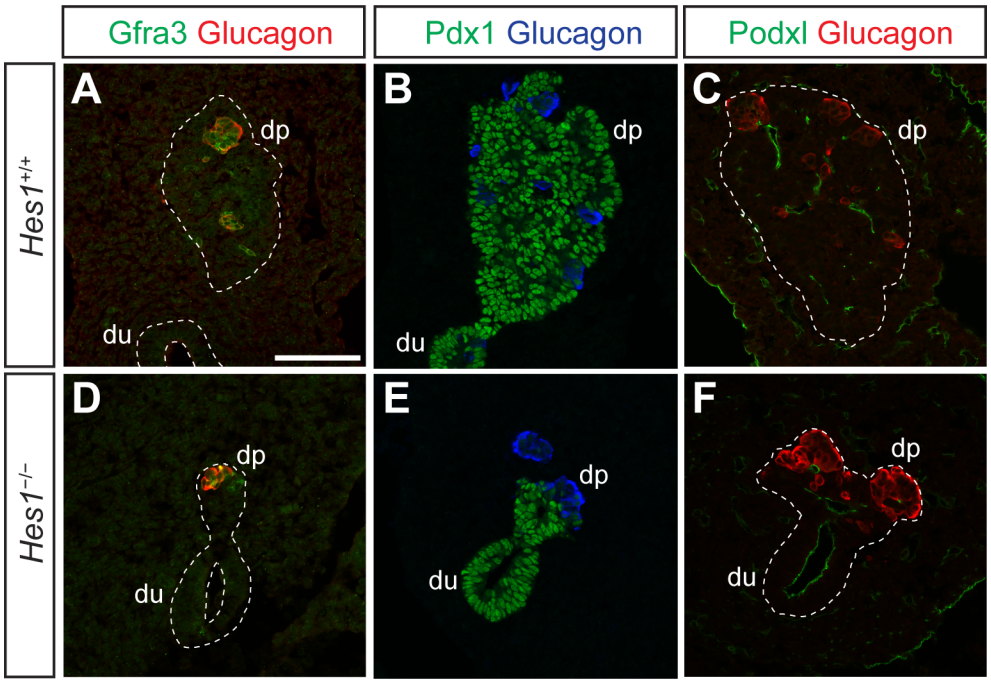

Fig. S5. Expression of Gfra3 and Podxl appear similar in *Hes1* mutants and controls. IF analysis of pancreas cross sections from E10.5 *Hes1*$^{+/+}$ (A-C) and *Hes1*$^{-/-}$ (D-F) showing Gfra3 and glucagon (A,D), Pdx1 and glucagon (B,E), or Podxl and glucagon (C,F). Dorsal is up. Near adjacent sections are shown. dp: dorsal pancreas, du: duodenum. Scale bar is 100 µm.

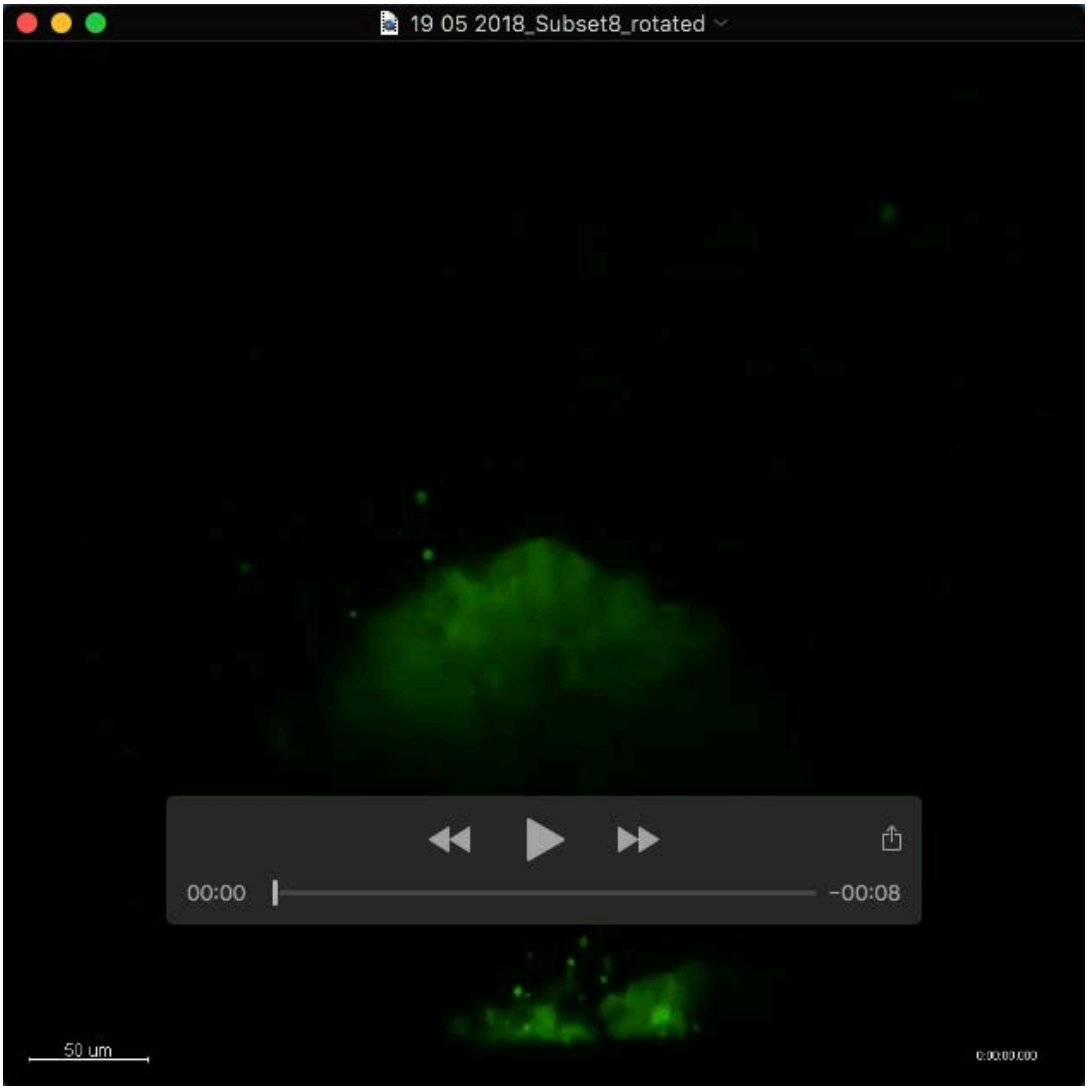

Movie S1. Growth of dorsal pancreas anlage in a *Hes1*$^{+/+}$ midgut explant. Live-imaging of the GFP expressing dorsal pancreatic cells during culture of the explanted midgut from an E9.5 *Hes1*$^{+/+}$*Pdx1*-GFP embryo. Anterior is to the left and dorsal is up.

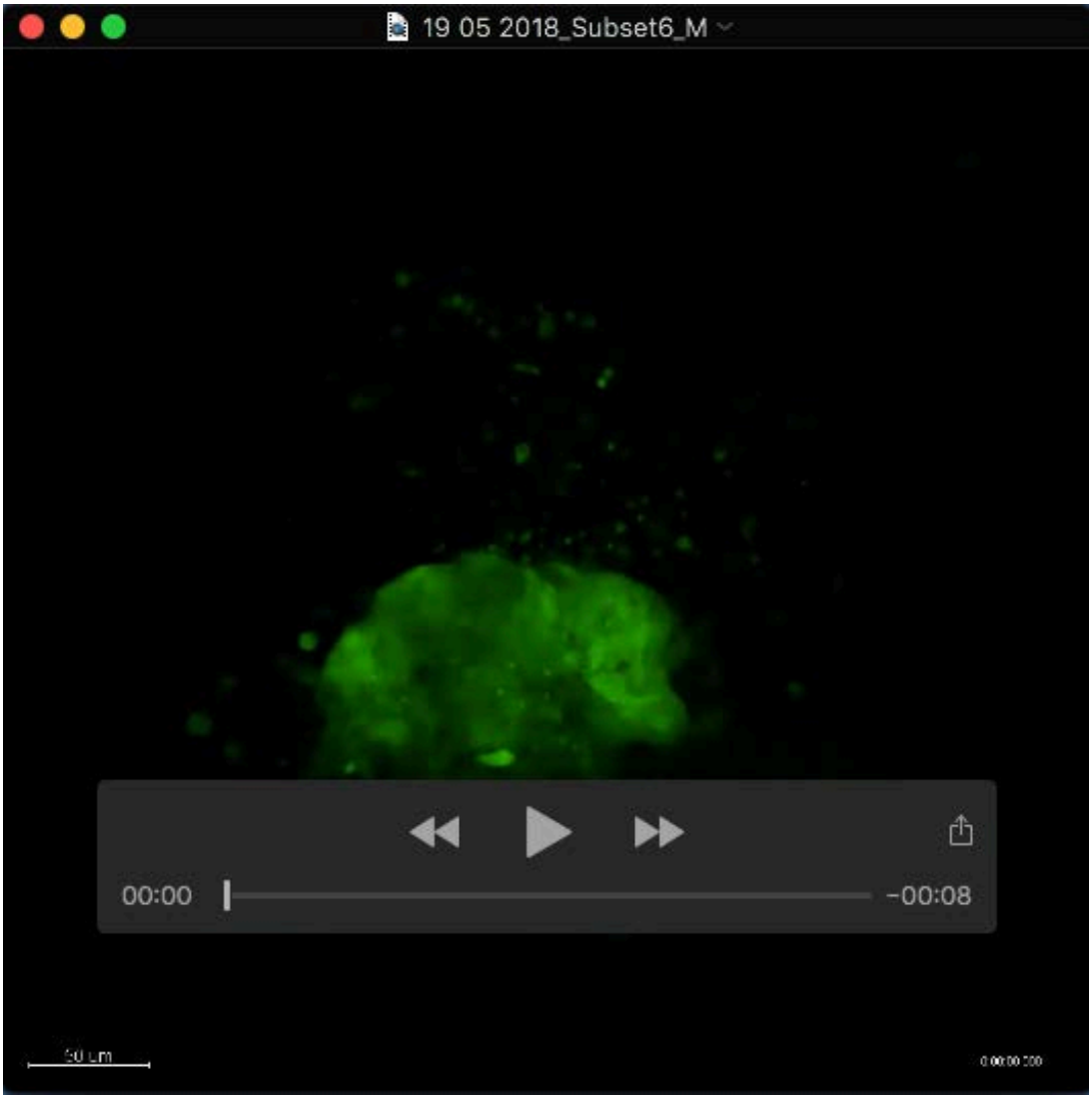

Movie S2. Growth of dorsal pancreas anlage in a *Hes1*$^{+/-}$ midgut explant. Live-imaging of the GFP expressing dorsal pancreatic cells during culture of the explanted midgut from an E9.5 *Hes1*$^{+/-}$*Pdx1*-GFP embryo. Anterior is to the left and dorsal is up.

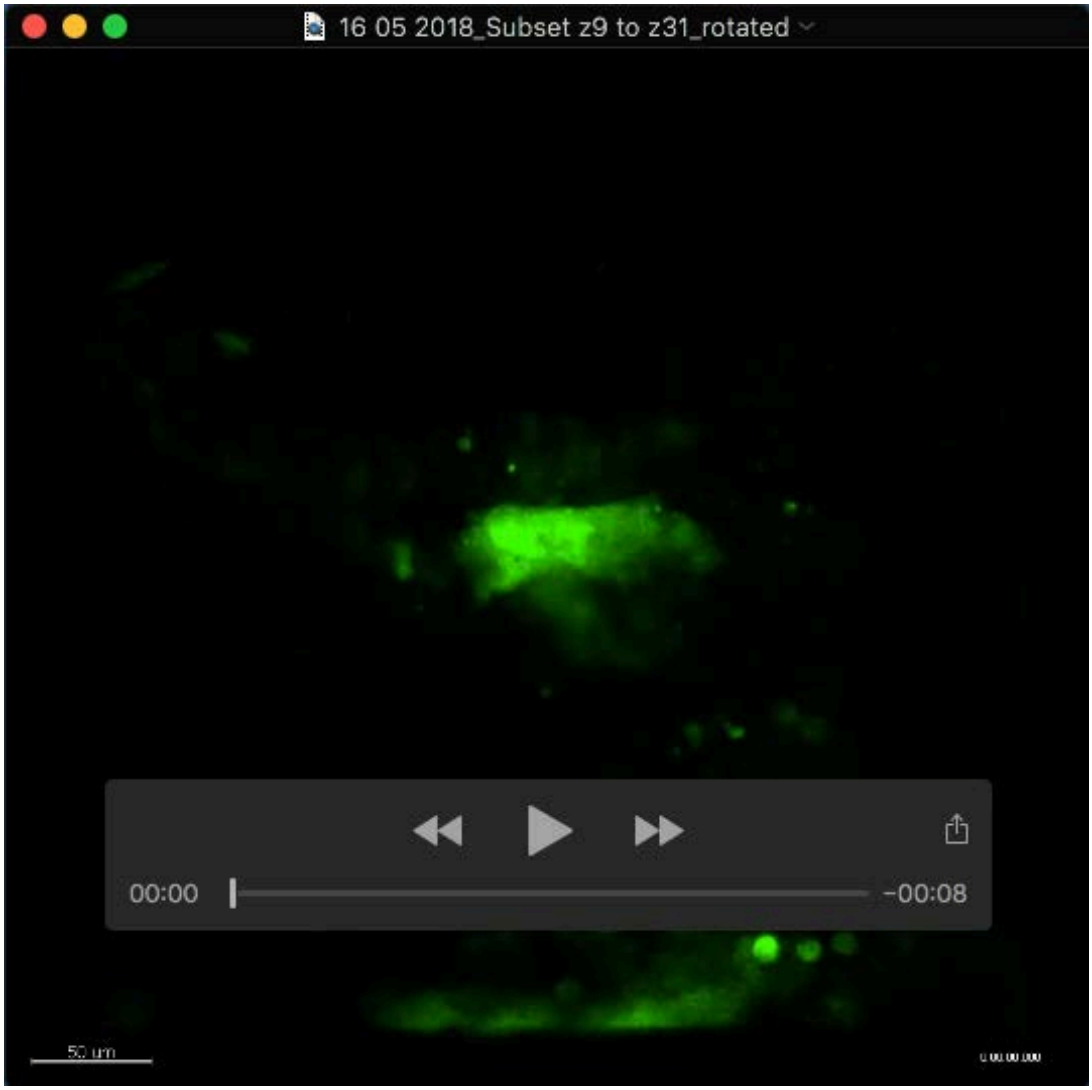

Movie 3. Rostral extension of the dorsal pancreas anlage in a *Hes1*$^{-/-}$ midgut explant. Live-imaging of the GFP expressing dorsal pancreatic cells during culture of the explanted midgut from an E9.5 *Hes1*$^{-/-}$*Pdx1*-GFP embryo. Note the lack of dorsal expansion and a rostral extension of the GFP^{+} cells. Anterior is to the left and dorsal is up.